

Sequential- and Parallel- Constrained Max-value Entropy Search via Information Lower Bound

Shion Takeno^{1,2}, Tomoyuki Tamura¹, Kazuki Shitara^{3,4}, and Masayuki Karasuyama¹

¹Nagoya Institute of Technology

²RIKEN Center for Advanced Intelligence Project

³Osaka University

⁴Japan Fine Ceramics Center

*takeno.s.mllab.nit@gmail.com, tomoyuki.tamura@nitech.ac.jp,
shitara@jwri.osaka-u.ac.jp, karasuyama@nitech.ac.jp*

Abstract

Bayesian optimization (BO) is known as a powerful tool for optimizing an unknown, expensive function through querying the function values sequentially. On the other hand, in many practical problems, additional unknown constraints also need to be considered. In this paper, we propose an information-theoretic approach called Constrained Max-value Entropy Search via Information lower BOund (CMES-IBO) for the constrained BO (CBO). Although information-theoretic methods have been studied in CBO literature, they have not revealed any relation between their acquisition functions and the original mutual information. In contrast, our acquisition function is an unbiased consistent estimator of a lower bound of mutual information. We show that our CMES-IBO has several advantageous properties such as non-negativity, estimation error bounds of the acquisition function, and well-definedness of the criterion, none of which have been shown for the existing information-theoretic CBO. Furthermore, by using conditional mutual information, we extend CMES-IBO to the parallel setting in which multiple queries can be issued simultaneously. We demonstrate the effectiveness of CMES-IBO by several benchmark functions.

1 Introduction

Bayesian optimization (BO) has been widely studied as an effective framework for the expensive black-box optimization problem. On the other hand, various real-world problems have additional unknown *constraints*. For example, materials discovery can be seen as an optimization of a physical property of materials, such as

conductivity, under constraints derived from other physical properties, such as stability. However, this task is often quite difficult because in many practical problems, measuring these properties comes at high cost, and further, functional forms of both of objective and constraint properties are unknown (black-box functions). To incorporate unknown constraint functions into BO, *constrained Bayesian optimization* (CBO) has also been studied [8, 9, 34, 35]. CBO tries to achieve the sample-efficient optimization by repeatedly observing values of objective and constraint functions that are estimated to be beneficial by an acquisition function.

We focus on information-theoretic approaches [14, 40, 41, 15, 18], whose superior performance have been repeatedly shown in BO and in its various extensions. Predictive Entropy Search (PES) [15] is one of the standard entropy-based BO methods, and the extension of PES to constrained optimization problems is called PES with Constraints (PESC) [16, 17]. PESC uses mutual information (MI) between a next observation and the optimal solution \mathbf{x}_* , but complicated approximations are required for the evaluation of MI. In contrast, Max-value Entropy Search (MES) [41] greatly facilitates computations compared with PES by using MI for the optimal value f_* . Perrone et al. [28] have proposed a direct extension of MES to CBO called constrained MES (cMES), but it is restricted to only one constraint. Moreover, they mainly focus on the binary setting, in which the binary value indicating feasibility (whether the queried point satisfies all the constraints or not) can only be observed. A more comprehensive review of related studies is shown in Section 5.

In this paper, we propose a novel information-theoretic CBO method called *Constrained Max-value Entropy Search via Information lower BOund* (CMES-IBO). CMES-IBO employs an estimator of a lower bound of MI between a querying point and f_* , unlike existing information-theoretic CBO methods in which any relation between their acquisition functions and the original MI has not been revealed. Compared with existing information-theoretic CBO methods, CMES-IBO can be motivated by a variety of desired properties such as (a) non-negativity, (b) unbiasedness and consistency to the lower bound, (c) a simple estimation error bound, and (d) well-definedness and interpretability for the infeasible case. For (a), non-negativity is obviously important because MI is non-negative while a naïve extension of MES can have a negative value. As listed in (b) and (c), we provide the theoretical analysis of our lower bound estimator. One of the significant consequences in this analysis is that a bound for the expected squared error between CMES-IBO and the true lower bound is derived as $2/K$, where K is the number of Monte Carlo samples. This simple bound enables us to assess the accuracy of the current lower bound estimation easily. A more important implication of this bound is that it guarantees the estimation accuracy without depending on variables such as the number of constraints and uncertainty of prediction models. For (d), in CBO, Bayes surrogate models (usually, Gaussian processes) can generate infeasible constraint functions, in which no solution satisfies constraints. In this case, MI even cannot be defined straightforwardly; nevertheless, existing information-theoretic CBO methods have ignored this issue. In our CMES-IBO, MI is always well-defined, and a clear interpretation of its behavior can be provided for the infeasibility issue.

Our main contributions are summarized as follows:

1. We develop an MI lower bound based CBO method called CMES-IBO, which is the first MES based

CBO method that can incorporate multiple constraints.

2. We derive the desirable properties of CMES-IBO (a)-(d) listed in the previous paragraph, and further, relations with the naïve extension of MES is also revealed.
3. We further develop a parallel extension of CMES-IBO, in which multiple queries can be issued simultaneously. The extension is based on a combination of the conditional MI and the greedy selection, for which we show that the estimation error can also be bounded by the same upper bound as the non-parallel case.

We demonstrate the effectiveness of CMES-IBO by various benchmark functions.

2 Preliminary

We are interested in the maximum value of the objective function $f : \mathcal{X} \mapsto \mathbb{R}$ under C constraint functions $g_c : \mathcal{X} \mapsto \mathbb{R}$ for $c = 1, \dots, C$, where $\mathcal{X} \subset \mathbb{R}^d$ is an input space. Let $\mathcal{X}_{\text{feasible}} := \{\mathbf{x} \mid g_c(\mathbf{x}) \geq z_c, c = 1, \dots, C\}$ be the feasible region, where $z_c \in \mathbb{R}$ is a given constant. The optimal solution of this constrained optimization problem is written as $\mathbf{x}_* := \arg \max_{\mathbf{x} \in \mathcal{X}_{\text{feasible}}} f(\mathbf{x})$. We consider the setting that the functions f and g_1, \dots, g_C are unknown but can be evaluated simultaneously for any given $\mathbf{x} \in \mathcal{X}$ with high observation cost. We assume that f and g_1, \dots, g_C follow independent *Gaussian processes* (GPs). Suppose that we already queried n points $\{(f(\mathbf{x}_i), g_1(\mathbf{x}_i), \dots, g_C(\mathbf{x}_i))\}_{i=1, \dots, n}$ for which actual observations can be contaminated with additive Gaussian noises. We write predictive distributions of $f(\mathbf{x})$ and $g_c(\mathbf{x})$ as $\mathcal{N}(\mu_n^{(f)}(\mathbf{x}), \sigma_n^{(f)^2}(\mathbf{x}))$ and $\mathcal{N}(\mu_n^{(g_c)}(\mathbf{x}), \sigma_n^{(g_c)^2}(\mathbf{x}))$, respectively. Since we use standard GP models, detailed definitions of these posteriors are omitted here (see Appendix A).

3 Constrained max-value entropy search via information lower bound

We here first derive CMES-IBO in Section 3.1, for which we show several advantageous properties in Section 3.2. The infeasibility issue and relations to existing MES-based approaches are also discussed in Section 3.3 and 3.4, respectively.

3.1 Acquisition function of CMES-IBO

Let

$$\mathbf{h}_{\mathbf{x}} := (f(\mathbf{x}), g_1(\mathbf{x}), \dots, g_C(\mathbf{x}))^{\top} \in \mathbb{R}^{C+1},$$

be a vector concatenating the objective and all the constraint functions, and f_* be the optimal value defined by

$$f_* := \begin{cases} \max_{\mathbf{x} \in \mathcal{X}_{\text{feasible}}} f(\mathbf{x}), & \text{if } \mathcal{X}_{\text{feasible}} \neq \emptyset, \\ \min_{\mathbf{x} \in \mathcal{X}} f(\mathbf{x}) - \zeta, & \text{otherwise,} \end{cases} \quad (1)$$

where $\zeta \geq 0$ is an arbitrary pre-specified constant. When the feasible region is empty, f_* is set as a value that must be worse than any other possible $f(\mathbf{x})$ in the domain \mathcal{X} . The parameter ζ represents a penalty for the infeasibility because larger ζ results in smaller f_* when $\mathcal{X}_{\text{feasible}} = \emptyset$. In later experiments, we set $\zeta \rightarrow \infty$, which means that infeasible solutions are maximally penalized (see Section 3.3 for detail). Suppose that we already have the dataset \mathcal{D}_{t-1} , which contains observations for the past $t-1$ queries. We consider selecting a next query \mathbf{x}_t by maximizing the MI between \mathbf{h}_x and f_* given \mathcal{D}_{t-1} :

$$\text{MI}(\mathbf{h}_x; f_* | \mathcal{D}_{t-1}). \quad (2)$$

Hereafter, we omit the conditioning by \mathcal{D}_{t-1} in MI, entropy, density, and probability when it is obvious from the context.

Since directly evaluating MI (2) is computationally intractable, we consider a lower bound derived as follows:

$$\begin{aligned} \text{MI}(\mathbf{h}_x; f_*) &= \mathbb{E}_{f_*} \left[\int p(\mathbf{h}_x | f_*) \log \frac{p(\mathbf{h}_x | f_*)}{p(\mathbf{h}_x)} d\mathbf{h}_x \right] \\ &= \mathbb{E}_{f_*} \left[\int p(\mathbf{h}_x | f_*) \log \frac{q(\mathbf{h}_x)}{p(\mathbf{h}_x)} d\mathbf{h}_x + D_{\text{KL}}(p(\mathbf{h}_x | f_*) || q(\mathbf{h}_x)) \right] \\ &\geq \mathbb{E}_{f_*} \left[\int p(\mathbf{h}_x | f_*) \log \frac{q(\mathbf{h}_x)}{p(\mathbf{h}_x)} d\mathbf{h}_x \right], \end{aligned} \quad (3)$$

where $D_{\text{KL}}(\cdot)$ is Kullback-Leibler divergence and $q(\mathbf{h}_x)$ is an arbitrary probability density function. See Appendix B for the derivation. This inequality can be seen as a special case of the variational lower bound [31]. The difference between the lower bound and MI is given as $\mathbb{E}_{f_*} [D_{\text{KL}}(p(\mathbf{h}_x | f_*) || q(\mathbf{h}_x))]$, and thus, the equality holds if $p(\mathbf{h}_x | f_*)$ is equal to $q(\mathbf{h}_x)$ for $\forall f_*$.

Let $\mathcal{A} := (f_*, \infty) \times (z_1, \infty) \times \dots \times (z_C, \infty) \subset \mathbb{R}^{C+1}$. To efficiently evaluate (3), we set $q(\mathbf{h}_x)$ as the following *truncated multivariate normal* (TMN) distribution:

$$q(\mathbf{h}_x) = p(\mathbf{h}_x | \mathbf{h}_x \in \bar{\mathcal{A}}) = \begin{cases} p(\mathbf{h}_x) / \Pr(\mathbf{h}_x \in \bar{\mathcal{A}}) & \text{for } \mathbf{h}_x \in \bar{\mathcal{A}}, \\ 0 & \text{for } \mathbf{h}_x \in \mathcal{A}, \end{cases} \quad (4)$$

where $\bar{\mathcal{A}} \subset \mathbb{R}^{C+1}$ is a complementary set of \mathcal{A} . A schematic illustration of $\mathbf{h}_x \in \bar{\mathcal{A}}$ for the one constraint case ($C = 1$) is shown in Fig. 1. When f_* is given, $f(\mathbf{x}) > f_*$ does not hold for any feasible \mathbf{x} , which is \mathbf{x} such that $g_1(\mathbf{x}) \geq z_1$ in the one constraint case. This indicates that \mathbf{h}_x cannot be in \mathcal{A} , and thus, the condition $\mathbf{h}_x \in \bar{\mathcal{A}}$ is obtained. In the original $p(\mathbf{h}_x | f_*)$, the condition $\mathbf{h}_{x'} \in \bar{\mathcal{A}}$ is imposed on $\forall \mathbf{x}' \in \mathcal{X}$, but it is replaced with conditioning only on the given \mathbf{x} in $q(\mathbf{h}_x)$. This replacement is inspired by existing entropy-based BO methods [e.g., 15, 41], in most of which the same type of replacements have been employed in a slightly different way (discussed in Section 3.4). Although the superior performance of the entropy-based

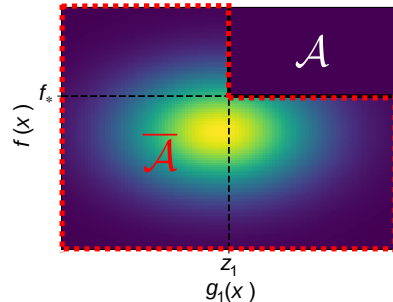


Figure 1: Schematic illustration of $\mathbf{h}_x \in \bar{\mathcal{A}}$ for $C = 1$. The horizontal and vertical axes express $g_1(\mathbf{x})$ and $f(\mathbf{x})$, respectively. The heatmap represents the density function $p(\mathbf{h}_x | \mathbf{h}_x \in \bar{\mathcal{A}}) = p(f(\mathbf{x}), g_1(\mathbf{x}) | \mathbf{h}_x \in \bar{\mathcal{A}})$ and the upper right area is \mathcal{A} . For a given f_* , the density should be 0 in \mathcal{A} , because $f(\mathbf{x})$ cannot be larger than f_* inside the feasible region $g(\mathbf{x}) \geq z_1$.

BO methods has been reported compared with other approaches, any relation between a criterion after this replacement and the original MI has not been revealed. On the other hand, the inequality (3) indicates that the rigorous lower bound can be obtained after this replacement.

By substituting TMN (4) into (3), we obtain our lower bound $L(\mathbf{x})$, in which the integral inside the expectation can be canceled out as follows:

$$L(\mathbf{x}) := \mathbb{E}_{f_*} \left[\int_{\bar{\mathcal{A}}} p(\mathbf{h}_{\mathbf{x}}|f_*) \log \frac{p(\mathbf{h}_{\mathbf{x}})/\Pr(\mathbf{h}_{\mathbf{x}} \in \bar{\mathcal{A}})}{p(\mathbf{h}_{\mathbf{x}})} d\mathbf{h}_{\mathbf{x}} \right] = \mathbb{E}_{f_*} [-\log \Pr(\mathbf{h}_{\mathbf{x}} \in \bar{\mathcal{A}})]. \quad (5)$$

See Appendix B for the detailed derivation. Since $\bar{\mathcal{A}}$ is not a simple hyperrectangle as shown in Fig. 1, the direct computation of $\Pr(\mathbf{h}_{\mathbf{x}} \in \bar{\mathcal{A}})$ is complicated when the number of constraints C is large. This difficulty can be avoided by using $\Pr(\mathbf{h}_{\mathbf{x}} \in \bar{\mathcal{A}}) = 1 - \Pr(\mathbf{h}_{\mathbf{x}} \in \mathcal{A})$. Evaluation of $\Pr(\mathbf{h}_{\mathbf{x}} \in \mathcal{A})$ is easier than $\Pr(\mathbf{h}_{\mathbf{x}} \in \bar{\mathcal{A}})$ because \mathcal{A} is a hyperrectangle. Let $Z := \Pr(\mathbf{h}_{\mathbf{x}} \in \mathcal{A})$. Because of the independence assumption, we see

$$Z = \Pr(f(\mathbf{x}) \geq f_*) \prod_{c=1}^C \Pr(g(\mathbf{x}) \geq z_c) = (1 - \Phi(\gamma_t^{(f)}(\mathbf{x}))) \prod_{c=1}^C (1 - \Phi(\gamma_t^{(g_c)}(\mathbf{x}))), \quad (6)$$

where $\gamma_t^{(f)}(\mathbf{x}) := (f_* - \mu_{t-1}^{(f)}(\mathbf{x}))/\sigma_{t-1}^{(f)}(\mathbf{x})$, $\gamma_t^{(g_c)}(\mathbf{x}) := (z_c - \mu_{t-1}^{(g_c)}(\mathbf{x}))/\sigma_{t-1}^{(g_c)}(\mathbf{x})$, and Φ is the cumulative distribution function (CDF) of the standard normal distribution. By applying the Monte Carlo approximation to \mathbb{E}_{f_*} in (5), we obtain the acquisition function of CMES-IBO as

$$\alpha_t^{\text{IBO}}(\mathbf{x}) = -\frac{1}{K} \sum_{f_* \in \mathcal{F}_*} \log(1 - Z), \quad (7)$$

where \mathcal{F}_* is a set of the sampled maximum f_* from the current GPs and $K = |\mathcal{F}_*|$.

To sample f_* , we employ an approach using the random Fourier feature (RFF) [32]. We first generate approximate sample paths of objective and constraint functions from Bayesian linear regression models using RFF, and then, we solve a (white-box) constrained optimization problem defined by the generated sample paths by using a general solver (see Appendix F.1 for details). A similar approach has been commonly employed in the entropy-based BO [41, 15]. Once we obtain \mathcal{F}_* , this acquisition function is obviously easy to compute because Z (6) can be calculated through the univariate Gaussian CDF. The algorithm for our CMES-IBO is shown in Appendix F. Although we mainly focus on the independent setting in this paper, CMES-IBO can easily apply to the correlated setting by computing $Z = \Pr(\mathbf{h} \in \mathcal{A})$ as the CDF of the multivariate (correlated) normal distribution. We evaluate the performance of the CMES-IBO on correlated synthetic functions in Appendix I.3.

3.2 Analytical properties of lower bound estimator

The acquisition function (7) has several desired properties. First, the Monte Carlo estimator (7), i.e., $a_t^{\text{IBO}}(\mathbf{x})$, is always non-negative, which is obvious from the definition of (7) and $Z \in [0, 1)$. This is essential because the acquisition function approximates the non-negative MI. Second, $a_t^{\text{IBO}}(\mathbf{x})$ is an unbiased consistent estimator of the rigorous lower bound $L(\mathbf{x})$ defined in (5). Unbiasedness here indicates $\mathbb{E}_{\mathcal{F}_*} [a_t^{\text{IBO}}(\mathbf{x})] = L(\mathbf{x})$ where $\mathbb{E}_{\mathcal{F}_*}$

is the expectation with respect to the sampling of \mathcal{F}_* , and consistency is $\lim_{K \rightarrow \infty} a_t^{\text{IBO}}(\mathbf{x}) = L(\mathbf{x})$. These are immediate consequences from properties of the Monte Carlo estimation but are important because existing entropy-based BO methods have not shown any relation between their acquisition functions and MI even if $K \rightarrow \infty$. Third, the estimation error with respect to the true lower bound $L(\mathbf{x})$ can be analyzed by the following theorem:

Theorem 3.1. *The expected squared error of the estimator (7) is bounded as $\mathbb{E}_{\mathcal{F}_*}[(\alpha_t^{\text{IBO}}(\mathbf{x}) - L(\mathbf{x}))^2] \leq 2/K$. Further, this derives an upper bound of the estimation error as $|\alpha_t^{\text{IBO}}(\mathbf{x}) - L(\mathbf{x})| \leq \sqrt{2/(\delta K)}$ with probability at least $1 - \delta$, where $\delta \in (0, 1)$.*

See Appendix C for the proof. This theorem provides a finite sample bound of $|\alpha_t^{\text{IBO}}(\mathbf{x}) - L(\mathbf{x})|$. Since both upper bounds are quite simple, we can easily assess the current accuracy of Monte Carlo estimation. Further, the rates of convergence only depend on K (and δ). This is not trivial because MI itself should depend on various quantities such as the number of constraints C and the predictive variances $\sigma_{t-1}^{(f)^2}$ and $\sigma_{t-1}^{(g_c)^2}$. However, Theorem 3.1 shows that the estimation error is bounded by using a surprisingly simple value without any dependence on these variables, which can be seen as a guarantee of the robustness of CMES-IBO.

3.3 Discussion on infeasibility

Particularly when the dataset \mathcal{D}_{t-1} does not contain any feasible solution (which typically occurs in the beginning of the optimization), it often occurs that a sample path generated for sampling f_* does not have any feasible solution. In our definition (1), f_* can be determined even in this infeasible case. We here discuss how our definition of f_* for $\mathcal{X}_{\text{feasible}} = \emptyset$ affects the behavior of CMES-IBO. For simplicity, we consider the case of $K = 1$. If the sample path does not have a feasible region, the acquisition function (7) becomes $-\log(1 - P_{\text{imp}} \times P_{\text{fea}})$, where $P_{\text{imp}} := \Pr(f(\mathbf{x}) \geq \min_{\mathbf{x} \in \mathcal{X}} f(\mathbf{x}) - \zeta)$ and $P_{\text{fea}} := \prod_{c=1}^C \Pr(g_c(\mathbf{x}) \geq z_c)$. In this criterion, P_{imp} and P_{fea} represent benefits for obtaining a larger value of $f(\mathbf{x})$ and for obtaining a feasible solution, respectively. Since now no feasible solution exists in the sample path, the gain of $f(\mathbf{x})$ is evaluated by comparing with a value smaller than the minimum value in \mathcal{X} . This enables us to incorporate the objective value $f(\mathbf{x})$ into a decision even only from one infeasible sample path.

On the other hand, by considering $\zeta \rightarrow \infty$, we can construct a simpler acquisition function that avoids computations of $\min_{\mathbf{x} \in \mathcal{X}} f(\mathbf{x})$. Then, since $P_{\text{imp}} = 1$ for $\forall \mathbf{x}$, only the probability of being feasible P_{fea} is maximized. Note that when $K > 1$, the setting $\zeta \rightarrow \infty$ still can incorporate the effect of the objective function through the frequency that sampled constraint functions have a feasible region. If the frequency is low, the probability of being feasible has a dominant effect, while if the frequency is high, the effect of the objective function becomes stronger. Note that sampled constraint functions can have feasible solutions even when the dataset \mathcal{D}_{t-1} does not contain any feasible solution.

3.4 Relation to existing max-value entropy search

Although we employ the lower bound based approach to derive CMES-IBO, Perrone et al. [28] have proposed a more direct extension of MES to CBO (Note that Perrone et al. [28] mainly focus on the binary setting, in which a binary value indicating feasible or not is only observed). However, their derivation is restricted to only one constraint ($C = 1$), and Fernández-Sánchez et al. [6] described that the extension to multiple constraints is not obvious. To consider the relation with CMES-IBO, we here extend this original MES-based approach to the multiple constraints case, which we refer to as CMES. In CMES, MI is approximated as

$$\begin{aligned} \text{MI}(\mathbf{h}_x; f_*) &= H(\mathbf{h}_x) - \mathbb{E}_{f_*} [H(\mathbf{h}_x | f_*)] \\ &\approx H(\mathbf{h}_x) - \mathbb{E}_{f_*} [H(\mathbf{h}_x | \mathbf{h}_x \in \bar{\mathcal{A}})] \end{aligned} \quad (8)$$

$$\approx \frac{1}{K} \sum_{f_* \in \mathcal{F}_*} \left\{ \frac{Z}{2(1-Z)} \left(\frac{\gamma_t^{(f)}(\mathbf{x}) \phi(\gamma_t^{(f)}(\mathbf{x}))}{1 - \Phi(\gamma_t^{(f)}(\mathbf{x}))} + \sum_{c=1}^C \frac{\gamma_t^{(g_c)}(\mathbf{x}) \phi(\gamma_t^{(g_c)}(\mathbf{x}))}{1 - \Phi(\gamma_t^{(g_c)}(\mathbf{x}))} \right) - \log(1-Z) \right\}, \quad (9)$$

where $H(\cdot)$ is the differential entropy and ϕ is the probability density function of the standard normal distribution. See Appendix D for the derivation. The first approximation (8) is the replacement from $p(\mathbf{h}_x | f_*)$ to $p(\mathbf{h}_x | \mathbf{h}_x \in \bar{\mathcal{A}})$ in the entropy of the second term, and the second approximation (9) is the Monte Carlo estimation of \mathbb{E}_{f_*} . About the replacement in the first approximation (8), CMES-IBO also replaces $p(\mathbf{h}_x | f_*)$ with $q(\mathbf{h}_x) = p(\mathbf{h}_x | \mathbf{h}_x \in \bar{\mathcal{A}})$ in (3), but an important difference is that (8) is not a lower bound of the original MI. In fact, any relation between (8) and the original MI has not been revealed so far, including the unconstrained MES. Therefore, even when $K \rightarrow \infty$ or taking an expectation with respect to \mathcal{F}_* , CMES is difficult to interpret unlike CMES-IBO. Further, the acquisition function (9) can be a negative value (an example is in Appendix D.3).

In addition, CMES can be seen as an approximation of CMES-IBO. Our lower bound $L(\mathbf{x})$ (5) can be transformed into $L(\mathbf{x}) = H(\mathbf{h}_x) - \mathbb{E}_{f_*} [\int -p(\mathbf{h}_x | f_*) \log p(\mathbf{h}_x | \mathbf{h}_x \in \bar{\mathcal{A}}) d\mathbf{h}_x]$. If we further replace $p(\mathbf{h}_x | f_*)$ with $p(\mathbf{h}_x | \mathbf{h}_x \in \bar{\mathcal{A}})$ in the second term, this equation is reduced to (8). This indicates that introducing an additional approximation to our lower bound criterion results in the conventional criterion (8). Another advantage of CMES-IBO compared with CMES is its simplicity of the acquisition function (7). The acquisition function of CMES (9) has an additional first term compared with CMES-IBO (7). Although CMES (9) is also easy to calculate, this first term has a complicated function form. The simplicity of CMES-IBO enables us to derive desirable properties such as non-negativity, the $2/K$ estimation variance, and the interpretability for the infeasible case. Further, this simplicity results in better computational efficiency of CMES-IBO in the correlated setting, though we do not particularly focus on this setting (with respect to the number of constraints C , the computational complexity of CMES-IBO is $O(C^2)$ in contrast to $O(C^4)$ of CMES for the correlated case as shown in Appendix F.2).

A notable difference of our study from [28] is that in [28], f_* is defined as $\max f(\mathbf{x})$, s.t. $g_c(\mathbf{x}) \geq z_c$ for $\forall c = 1, \dots, C$, by which the infeasible case is not considered. We emphasize that GPs usually can generate an infeasible sample path, i.e., $\Pr(\mathcal{X}_{\text{feasible}} = \emptyset) > 0$ (in fact, this is always the case unless we observe a

noiseless feasible solution). Then, there is a possibility that f_* is not defined, by which MI even cannot be theoretically defined. Other than using our definition of f_* (1), another possible approach to avoiding this problem is to assume the existence of feasible solutions in the GPs, but it causes at least the following two computational difficulties. First, we need to generate sample paths that have feasible solutions for sampling f_* . A naïve approach is the rejection sampling, in which generated constraint functions are rejected if no feasible solution exists, but this may require a huge number of samplings. Second, the predictive distribution of $\mathbf{h}_{\mathbf{x}}$ under this condition $p(\mathbf{h}_{\mathbf{x}} \mid \text{at least one feasible } \mathbf{x} \text{ exists})$ is not a Gaussian distribution anymore, and is analytically intractable. This makes the entire computational procedures of both CMES-IBO and CMES much more complicated. Perrone et al. [28] did not mention the above issues at all and used the usual predictive distributions of GPs in the entire acquisition function evaluation without any justification. Our definition of f_* resolves the above issues and provides a clear interpretation as we discussed in Section 3.3. Note that the same problem exists in the PES-based CBO [16, 17].

Finally, we describe the relation to the unconstrained MES. The original MES paper [41] showed that MES is equivalent to the maximization of $\Pr(f(\mathbf{x}) \geq f_*)$ when $K = 1$. In the case of CMES-IBO, maximizing the acquisition function (7) is equivalent to maximizing $\Pr(f(\mathbf{x}) \geq f_*, g_c(\mathbf{x}) \geq z_c \text{ for } \forall c)$ when $K = 1$. This can be easily derived from the monotonicity of logarithm and the definition of Z (6). This behavior of CMES-IBO obviously can be seen as a constraint counterpart of the unconstrained MES, while CMES does not have this property.

4 Parallelization

In this section, we consider a parallel extension of CMES-IBO. We assume that Q workers are available by which we can select Q queries as a batch at every iteration. Let $\mathcal{X}_q := \{\mathbf{x}^{(1)}, \dots, \mathbf{x}^{(q)}\}$ be a set of input queries and $\mathcal{H}_q := \{\mathbf{h}_{\mathbf{x}^{(1)}}, \dots, \mathbf{h}_{\mathbf{x}^{(q)}}\}$ be a set of output vectors for an integer $1 \leq q \leq Q$. A naïve extension is to maximize MI between \mathcal{H}_Q and f_* , i.e., $\text{MI}(\mathcal{H}_Q; f_*)$, with respect to the queries \mathcal{X}_Q . However, this approach results in a Qd dimensional acquisition function maximization, which is often extremely hard. Instead, we propose a greedy approximation of $\max_{\mathcal{X}_Q} \text{MI}(\mathcal{H}_Q; f_*)$ using the *conditional mutual information* (CMI).

The q -th step of our greedy selection is defined as $\arg \max_{\mathbf{x}^{(q)}} \text{MI}(\mathcal{H}_q; f_*)$, where $\mathbf{x}^{(1)}, \dots, \mathbf{x}^{(q-1)}$ are already fixed by the previous steps. This procedure maximizes the additional information gain produced by $\mathbf{h}_{\mathbf{x}^{(q)}}$, which can be seen through the following expansion:

$$\text{MI}(\mathcal{H}_q; f_*) = \text{MI}(\mathcal{H}_{q-1}; f_*) + \text{CMI}(\mathbf{h}_{\mathbf{x}^{(q)}}; f_* | \mathcal{H}_{q-1}),$$

where the second term is $\text{CMI}(\mathbf{h}_{\mathbf{x}^{(q)}}; f_* | \mathcal{H}_{q-1}) := \mathbb{E}_{\mathcal{H}_{q-1}} [\text{MI}(\mathbf{h}_{\mathbf{x}^{(q)}}; f_* | \mathcal{H}_{q-1})]$. Importantly, the first term does not depend on $\mathbf{x}^{(q)}$ anymore. Therefore, we obtain $\arg \max_{\mathbf{x}^{(q)}} \text{MI}(\mathcal{H}_q; f_*) = \arg \max_{\mathbf{x}^{(q)}} \text{CMI}(\mathbf{h}_{\mathbf{x}^{(q)}}; f_* | \mathcal{H}_{q-1})$, which means that the greedy selection can be performed by the maximization of CMI.

Our lower bound approach used in (5) can be applied to CMI as follows:

$$\text{CMI}(\mathbf{h}_{\mathbf{x}^{(q)}}; f_* | \mathcal{H}_{q-1}) \geq -\mathbb{E}_{\mathcal{H}_{q-1}, f_*} [\log(1 - Z_q)] =: L_{\text{par}}(\mathbf{x}^{(q)}), \quad (10)$$

where $Z_q := \Pr(\mathbf{h}_{\mathbf{x}^{(q)}} \in \mathcal{A} | \mathcal{X}_{q-1}, \mathcal{H}_{q-1})$. See Appendix B for the derivation. Suppose that $m_q^{(f)}(\mathbf{x})$ and $s_q^{(f)^2}(\mathbf{x})$ are the predictive mean and variance of $f(\mathbf{x})$ after conditioning by \mathcal{H}_{q-1} , respectively, and that $m_q^{(g_c)}(\mathbf{x})$ and $s_q^{(g_c)^2}(\mathbf{x})$ are those for $g_c(\mathbf{x})$. Then, from the independence assumption, $Z_q = (1 - \Phi(\eta_q^{(f)}(\mathbf{x}^{(q)}))) \prod_{c=1}^C (1 - \Phi(\eta_q^{(g_c)}(\mathbf{x}^{(q)})))$, where $\eta_q^{(f)}(\mathbf{x}^{(q)}) = (f_* - m_q^{(f)}(\mathbf{x}^{(q)})) / s_q^{(f)}(\mathbf{x}^{(q)})$ and $\eta_q^{(g_c)}(\mathbf{x}^{(q)}) = (z_c - m_q^{(g_c)}(\mathbf{x}^{(q)})) / s_q^{(g_c)}(\mathbf{x}^{(q)})$, $c = 1, \dots, C$. By applying the Monte Carlo estimation to the expectation in (10), we obtain the acquisition function for the q -th query as

$$\alpha_t^{\text{IBO}}(\mathbf{x}^{(q)} | \mathcal{X}_{q-1}) = -\frac{1}{K} \sum_{(f_*, \mathcal{H}_{q-1}) \in \mathcal{J}} \log(1 - Z_q), \quad (11)$$

where \mathcal{J} is a set of K sampled (f_*, \mathcal{H}_{q-1}) from the current GPs. Note that jointly sampling f_* and \mathcal{H}_{q-1} can be easily performed by almost the same procedure as the sequential case (see Appendix F.1 for detail). Given \mathcal{J} , our parallel extension is also shown as a closed-form and possible to compute stably. We present the general algorithm for sequential- and parallel- CMES-IBO in Appendix F. Note that for CMES, a similar parallelization is also possible (see Appendix D.2), but here again, the relation with the original MI is unclear, as we discussed in Section 3.4.

Our parallel acquisition function (11) inherits desirable properties of CMES-IBO. First, since $Z_q \in [0, 1)$, non-negativity still obviously holds. Second, unbiasedness $\mathbb{E}_{\mathcal{J}}[\alpha_t^{\text{IBO}}(\mathbf{x}^{(q)} | \mathcal{X}_{q-1})] = L_{\text{par}}(\mathbf{x}^{(q)})$ where $\mathbb{E}_{\mathcal{J}}$ is the expectation with respect to the sampling of \mathcal{J} , and consistency $\lim_{K \rightarrow \infty} \alpha_t^{\text{IBO}}(\mathbf{x}^{(q)} | \mathcal{X}_{q-1}) = L_{\text{par}}(\mathbf{x}^{(q)})$ are guaranteed by the Monte Carlo estimation. Third, Theorem 3.1 can be extended to the parallel setting as below:

Theorem 4.1. *The expected squared error of the estimator (11) is bounded as $\mathbb{E}_{\mathcal{J}}[(\alpha_t^{\text{IBO}}(\mathbf{x}^{(q)} | \mathcal{X}_{q-1}) - L_{\text{par}}(\mathbf{x}^{(q)}))^2] \leq 2/K$. Further, this derives an upper bound of the estimation error as $|\alpha_t^{\text{IBO}}(\mathbf{x}^{(q)} | \mathcal{X}_{q-1}) - L_{\text{par}}(\mathbf{x}^{(q)})| \leq \sqrt{2/(\delta K)}$ with probability at least $1 - \delta$, where $\delta \in (0, 1)$.*

See Appendix C for the proof. Both bounds are equal to the case of the sequential querying. The Monte Carlo approximation of the expectation $\mathbb{E}_{\mathcal{H}_{q-1}, f_*}$ in (10) may seem difficult because of its dimension $(q-1)(C+1)+1$. However, this theorem indicates that even if the number of queries Q increases, the stability of the estimator can be guaranteed because the bounds do not depend on q .

5 Related work

Extensions of unconstrained BO methods to CBO have been widely studied. *Expected Improvement with Constraint* (EIC) [34, 35, 9, 8] is based on the standard EI [26]. However, the expected improvement cannot be defined without obtaining a feasible solution because no ‘current best solution’ is defined. Gelbart et al.

[9] proposed maximizing the probability of being feasible in this case, but this strategy does not take the prediction of the objective function into account. Letham et al. [22] replaced the current best value in EI with a hyperparameter M when no feasible observation exists. This parameter balances the exploit-exploration tradeoff, but no reasonable selection strategy for M has been provided. Gramacy and Lee [12], and Picheny [29] consider the expected reduction of the expectation and probability of improvement, respectively. However, since these approaches require expensive numerical integrations depending on the input dimension d , their applicability is severely limited. *Thompson Sampling* (TS) is another standard approach in BO, based on which *Scalable Constrained Bayesian Optimization* (SCBO) [5] has been proposed for CBO recently. Unlike the standard TS, which can be justified by strong theoretical results [21], the convergence rate for the regret of SCBO has not been shown.

Several methods have been derived from classical constrained optimization algorithms. Gramacy et al. [13], and Picheny et al. [30] used a GP as a surrogate of the augmented Lagrangian (AL) function. In these AL-based methods, the initial values of a Lagrange multiplier and a penalty coefficient should be specified. In the case of the ‘known’ objective and constraints setting of the classical numerical optimization, AL-based methods are robust with respect to these settings because these values are refined during a large number of iterations. However, for the expensive black-box optimization, the effect of the initial parameters is not negligible because the number of possible iterations is much smaller than the classical optimization. Ariafar et al. [1] proposed *Alternating Direction Method of Multipliers Bayesian Optimization* (ADMMBO) based on the famous ADMM algorithm. However, ADMMBO is only for *decoupled setting*, in which each one of objective and constraint functions is observed separately. In this paper, we only focus on the setting in which objective and constraint functions are simultaneously observed.

Entropy-based approaches are also studied in CBO literature. Hernández-Lobato et al. [16, 17] proposed *Predictive Entropy Search with Constraint* (PESC) which is based on PES for the unconstrained problem [15]. PESC considers the information gain of \mathbf{x}_* under the constraints, which is a measure of global utility and does not require any additional hyperparameters. However, PESC performs complicated approximations for which any relation with the original MI has not been clarified. Another well-known entropy-based BO is MES, for which we already discussed in Section 3.4. MES for multi-objective optimization with constraints has been recently proposed by two papers [3, 6]. Fernández-Sánchez et al. [6] pointed out that the entropy evaluation of [3] is obviously incorrect and further showed that the performance is inferior to the random search. Fernández-Sánchez et al. [6] use the assumed density filtering for extending MES, but this approach results in complicated approximations by which the simplicity of the original MES is not maintained anymore.

In addition, by using CMI, we extend CMES-IBO (and CMES) to the parallel setting, which is made possible by the wide applicability and computational simplicity of MES. The parallel extension of CBO has not been widely studied. Letham et al. [22] have proposed the parallel extension of EIC for noisy observations using the quasi-Monte Carlo method. SCBO [5] is also applicable to the parallel setting easily because of the nature of TS. These approaches inherit the difficulties of their sequential counterparts mentioned in

this section. On the other hand, for the context of multi-fidelity BO, a parallel extension of MES has been proposed by [39]. Although this also employs CMI, the acquisition function is not a lower bound of CMI, and constrained problems have not been studied. Wilson et al. [42] discussed the Monte Carlo based parallel BO in general, but they considered only ‘myopic maximal (MM) acquisition functions’ for the unconstrained BO. MES is not included in a class of MM acquisition functions, and CBO was not considered in [42] at all.

To our knowledge, no existing studies use a lower bound of MI for BO. An approach recently proposed by Moss et al. [27] considers a lower bound based extension of MES. However, their bound is a lower bound of the ‘approximate’ MI used in the original MES, which is not a lower bound of MI. Therefore, the basic ideas are obviously different, and constrained problems have not been studied in [27]. Although we only focus on constrained problems in this paper, a similar lower bound can be derived even for the unconstrained case. Considering the effectiveness of the lower bound approach for the unconstrained problem is one of our important future works.

Lastly, we mention convergence analysis of the entropy-based BO. Wang and Jegelka [41] show the regret analysis of ‘one sample MES,’ in which only one optimal value is sampled in the Monte Carlo approximation. To our knowledge, except for this, no other regret analysis is known for the entropy-based BO ([2] shows an extension to the multi-objective problem, but their regret can be negative value as pointed out by [37]). However, we find that the original theorem of MES contains several critical flaws. For example, the theorem assumes that f follows a GP, but the maximum of f is regarded as a deterministic variable in the proof (more details including other issues are in Appendix G). Therefore, convergence guarantee is still an open problem for the entropy-based BO.

6 Experiments

We demonstrate the performance of sequential optimization by comparing with CMES, EIC [9], a TS-based method referred to as TSC, and PESC [16] (in Spearmint at <https://github.com/HIPS/Spearmint/tree/PESC> under an Academic and Non-Commercial Research Use License). Note that CMES is based on our definition of f_* (1). TSC is a variant of SCBO [5] simplified by omitting the output transformation (such as the Gaussian copula-based transformation of the objective) and the trust region strategy. Since these two are general strategies applicable to any acquisition functions, to only focus on the difference of acquisition functions, we do not employ them. Although the AL-based methods [13, 30] are not shown as baselines, they are outperformed by PESC and SCBO in prior work [16, 5], respectively.

For the parallel setting, although Letham et al. [22] proposed the parallel extension of EIC, they particularly focus on the case that the noise level is quite high, in which other approaches degrade in performance. This extreme setting is not our main interest, and therefore, we devise a simpler extension of the Monte Carlo based parallel EI [36] to the constraint setting with the idea of ‘plugged-in’ parameter M [22] described in Section 5. We also parallelize TSC by sampling \mathbf{x}_* from the GPs Q times. The prefix ‘P-’ indicates a

parallelized variant of each method (e.g., P-EIC and P-CMES).

We evaluate the performance using the *utility gap*, which is also employed in various prior work [16, 30, 5]. We set the recommendation at iteration t as $\hat{\mathbf{x}}_t = \max_{\mathbf{x} \in \mathcal{X}} \mu_{t-1}^{(f)}(\mathbf{x})$, s.t. $\forall c, \Pr(g_c(\mathbf{x}) \geq z_c) \geq \sqrt[3]{0.95}$. Then, the utility gap is defined as $f_* - f(\hat{\mathbf{x}}_t)$ if the recommendation is feasible, otherwise $f_* - \min_{\mathbf{x} \in \mathcal{X}} f(\mathbf{x})$, which indicates that an infeasible recommendation results in the worst utility gap. The initial inputs are sampled by Latin hypercube sampling [24]. The sample size of all Monte Carlo approximations is set as 10. For the parallel querying, we set $Q = 3$. For the kernel function in all GPs, we used a linear combination of the linear kernel $k_{\text{LIN}} : \mathcal{X} \times \mathcal{X} \rightarrow \mathbb{R}$ and RBF kernel $k_{\text{RBF}} : \mathcal{X} \times \mathcal{X} \rightarrow \mathbb{R}$ defined as $\sigma_{\text{LIN}}^2 k_{\text{LIN}}(\mathbf{x}, \mathbf{x}') + \sigma_{\text{RBF}}^2 k_{\text{RBF}}(\mathbf{x}, \mathbf{x}')$, where σ_{LIN}^2 and σ_{RBF}^2 are updated by the marginal likelihood maximization every 5 iteration. We report the mean and the standard error of the results obtained across 10 random initialization. For PESC, due to difficulty in rewriting the Spearmint specification, the default settings of kernels and inner optimization are used. Although PESC has the same number of initial points, their location is not identical to other methods because of the same reason. The infeasibility penalty ζ in CMES-IBO and CMES is set as $\zeta \rightarrow \infty$. Other experimental details are shown in Appendix H.

Evaluation on small C problems We first show results on the problems with one or two constraints. We used benchmark functions in CBO literature [8, 16]. The detailed form of each function is in Appendix H. The number of the initial points is set as $5d$ for the Hartmann6 function and 5 for the others. Gardner1 and Gardner2 are from [8]. Gardner1 is a simple test problem constructed by sine and cosine functions. Gardner2 also has a simple form, but its feasible region is tiny. The Gramacy function is from [13], which has multiple constraints ($C = 2$). The Hartmann6 function is used in [22], which has relatively high input dimension ($d = 6$). In all the results of Fig. 2, CMES-IBO is superior or comparable to the other methods. In Gardner1, the utility gap of CMES-IBO converged clearly faster than the other methods. In Gardner2, CMES-IBO and CMES showed superior performance than the other methods, which suggests that even when the feasible region is tiny, methods based on our MI effectively explored the search space. In Hartmann6, CMES-IBO and CMES showed larger decreases of the utility gaps than the other methods, and in particular, CMES-IBO shows a much faster decrease. We also show results on the parallel setting in Appendix I.

Evaluation on large C problems We here employed benchmark problems called G7 ($C = 8$ and $d = 8$) and G10 ($C = 6$ and $d = 10$), for which the detailed definitions can be found in [23]. In CBO literature, empirical evaluations are typically performed with $C \leq 2$, and thus, the settings $C = 8$ and 6 are relatively large. Moreover, the input dimension d is also large, and the estimated ratio between the feasible region and the input space is very small (less than 0.001%) [23]. The results for both of the sequential and parallel settings are shown in Fig. 3, in which the number of initial points is set as 10. We can see that CMES-IBO has superior or comparable to the other methods in all the plots. Note that the slow convergence of PESC can be because Spearmint does not employ the linear kernel even though these test functions contain linear functions. In G7, although the utility gaps of CMES and P-CMES were not lower than about 10, CMES-IBO

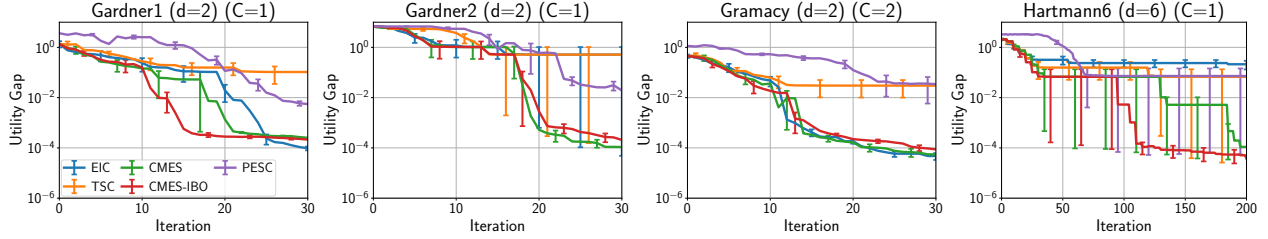


Figure 2: Utility gap of benchmark functions (average and standard error).

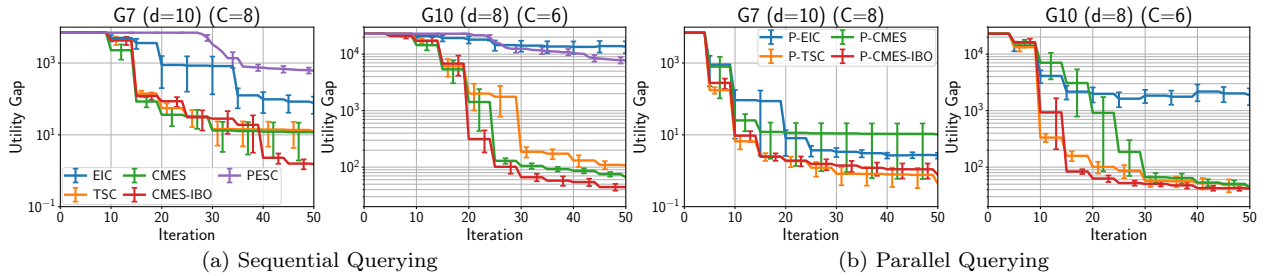


Figure 3: Utility gap of G7 and G10 functions (average and standard error).

converged to lower values. CMES-IBO also outperformed CMES clearly in both of sequential- and parallel-querying of G10. Results on other benchmark problems with $C = 4, 6$, and 9 from [23] are also shown in Appendix I.

7 Conclusion

In this paper, we proposed an information-theoretic constrained Bayesian optimization method called CMES-IBO, which is based on the lower bound of the MI. We further show its several desired properties such as non-negativity, unbiasedness and consistency to the lower bound, the bounds of the estimation error, and the interpretation about the infeasible case. Moreover, we extended CMES-IBO to the parallel setting, for which we showed that the error bounds are inherited. The effectiveness of our proposed method was shown through various benchmark functions.

Acknowledgments

This work was supported by MEXT/JSPS KAKENHI 17H04694, 21H03498, 18K04700, JP21J14673, and RIKEN Junior Research Associate Program.

References

- [1] Setareh Ariafar, Jaume Coll-Font, Dana Brooks, and Jennifer Dy. ADMMBO: Bayesian optimization with unknown constraints using ADMM. *Journal of Machine Learning Research*, 20(123):1–26, 2019.

- [2] Syrine Belakaria, Aryan Deshwal, and Janardhan Rao Doppa. Max-value entropy search for multi-objective Bayesian optimization. In *Advances in Neural Information Processing Systems 32*, pages 7825–7835. Curran Associates, Inc., 2019.
- [3] Syrine Belakaria, Aryan Deshwal, and Janardhan Rao Doppa. Max-value entropy search for multi-objective Bayesian optimization with constraints. *arXiv:2009.01721*, 2020.
- [4] Thomas M. Cover and Joy A. Thomas. *Elements of Information Theory*. Wiley-Interscience, 2006.
- [5] David Eriksson and Matthias Poloczek. Scalable constrained Bayesian optimization. In *Proceedings of The 24th International Conference on Artificial Intelligence and Statistics*, volume 130, pages 730–738. PMLR, 2021.
- [6] Daniel Fernández-Sánchez, Eduardo C. Garrido-Merchán, and Daniel Hernández-Lobato. Max-value entropy search for multi-objective Bayesian optimization with constraints. *arXiv:2011.01150*, 2020.
- [7] Manjunath B G and Stefan Wilhelm. Moments calculation for the doubly truncated multivariate normal density. *arXiv:1206.5387*, 2012.
- [8] Jacob Gardner, Matt Kusner, Zhixiang, Kilian Weinberger, and John Cunningham. Bayesian optimization with inequality constraints. In *Proceedings of the 31st International Conference on Machine Learning*, volume 32, pages 937–945. PMLR, 2014.
- [9] Michael A. Gelbart, Jasper Snoek, and Ryan P. Adams. Bayesian optimization with unknown constraints. In *Proceedings of the 30th Conference on Uncertainty in Artificial Intelligence*, page 250–259. AUAI Press, 2014.
- [10] Alan Genz. Numerical computation of multivariate normal probabilities. *Journal of Computational and Graphical Statistics*, 1:141–150, 1992.
- [11] GPy. GPy: A Gaussian process framework in python. <http://github.com/SheffieldML/GPy>, since 2012.
- [12] Robert Gramacy and Herbert Lee. Optimization under unknown constraints. *Bayesian Statistics 9*, 2010.
- [13] Robert B. Gramacy, Genetha A. Gray, Sébastien Le Digabel, Herbert K. H. Lee, Pritam Ranjan, Garth Wells, and Stefan M. Wild. Modeling an augmented Lagrangian for blackbox constrained optimization. *Technometrics*, 58(1):1–11, 2016.
- [14] Philipp Hennig and Christian J. Schuler. Entropy search for information-efficient global optimization. *Journal of Machine Learning Research*, 13(57):1809–1837, 2012.

- [15] José Miguel Hernández-Lobato, Matthew W. Hoffman, and Zoubin Ghahramani. Predictive entropy search for efficient global optimization of black-box functions. In *Advances in Neural Information Processing Systems 27*, page 918–926. Curran Associates, Inc., 2014.
- [16] José Miguel Hernández-Lobato, Michael A. Gelbart, Matthew W. Hoffman, Ryan P. Adams, and Zoubin Ghahramani. Predictive entropy search for Bayesian optimization with unknown constraints. In *Proceedings of the 32th International Conference on Machine Learning*, volume 37, pages 1699–1707. PMLR, 2015.
- [17] José Miguel Hernández-Lobato, Michael A. Gelbart, Ryan P. Adams, Matthew W. Hoffman, and Zoubin Ghahramani. A general framework for constrained Bayesian optimization using information-based search. *Journal of Machine Learning Research*, 17(160):1–53, 2016.
- [18] Matthew W. Hoffman and Zoubin Ghahramani. Output-space predictive entropy search for flexible global optimization. In *NIPS Workshop on Bayesian Optimization*, 2015.
- [19] William C. Horrace. Some results on the multivariate truncated normal distribution. *Journal of Multivariate Analysis*, 94(1):209–221, 2005.
- [20] Steven G. Johnson. The NLOpt nonlinear-optimization package. <http://github.com/stevengj/nlopt>, since 2008.
- [21] Kirthevasan Kandasamy, Akshay Krishnamurthy, Jeff Schneider, and Barnabas Póczos. Parallelised Bayesian optimisation via Thompson sampling. In *Proceedings of the 21st International Conference on Artificial Intelligence and Statistics*, volume 84, pages 133–142. PMLR, 2018.
- [22] Benjamin Letham, Brian Karrer, Guilherme Ottoni, and Eytan Bakshy. Constrained Bayesian optimization with noisy experiments. *Bayesian Anal.*, 14(2):495–519, 2019.
- [23] Jing Liang, Thomas Runarsson, Efrén Mezura-Montes, M. Clerc, Ponnuthurai Suganthan, Carlos Coello, and Kalyan Deb. Problem definitions and evaluation criteria for the CEC 2006 special session on constrained real-parameter optimization. *Nanyang Technological University, Tech. Rep*, 41, 2006.
- [24] Wei-Liem Loh. On Latin hypercube sampling. *Ann. Statist.*, 24(5):2058–2080, 1996.
- [25] Joseph Victor Michalowicz, Jonathan M. Nichols, and Frank Bucholtz. *Handbook of Differential Entropy*. Chapman and Hall/CRC, 2014.
- [26] Jonas Mockus, Vytautas Tiesis, and Antanas Zilinskas. The application of Bayesian methods for seeking the extremum. *Towards Global Optimization*, 2(117-129):2, 1978.
- [27] Henry B. Moss, David S. Leslie, Javier Gonzalez, and Paul Rayson. GIBBON: General-purpose information-based Bayesian optimisation. *arXiv:2102.03324*, 2021.

- [28] Valerio Perrone, Iaroslav Shcherbatyi, Rodolphe Jenatton, Cedric Archambeau, and Matthias Seeger. Constrained Bayesian optimization with max-value entropy search. *arXiv:1910.07003*, 2019.
- [29] Victor Picheny. A Stepwise uncertainty reduction approach to constrained global optimization. In *Proceedings of the 17th International Conference on Artificial Intelligence and Statistics*, volume 33, pages 787–795. PMLR, 2014.
- [30] Victor Picheny, Robert B Gramacy, Stefan Wild, and Sebastien Le Digabel. Bayesian optimization under mixed constraints with a slack-variable augmented Lagrangian. In *Advances in Neural Information Processing Systems 29*, pages 1435–1443. Curran Associates, Inc., 2016.
- [31] Ben Poole, Sherjil Ozair, Aaron Van Den Oord, Alex Alemi, and George Tucker. On variational bounds of mutual information. In *Proceedings of the 36th International Conference on Machine Learning*, volume 97, pages 5171–5180. PMLR, 2019.
- [32] Ali Rahimi and Benjamin Recht. Random features for large-scale kernel machines. In *Advances in Neural Information Processing Systems 20*, pages 1177–1184. Curran Associates, Inc., 2008.
- [33] Carl Edward Rasmussen and Christopher K. I. Williams. *Gaussian Processes for Machine Learning (Adaptive Computation and Machine Learning)*. The MIT Press, 2005.
- [34] Matthias Schonlau, William J. Welch, and Donald R. Jones. *Global versus local search in constrained optimization of computer models*, volume 34 of *Lecture Notes–Monograph Series*, pages 11–25. Institute of Mathematical Statistics, 1998.
- [35] Jasper Snoek. *Bayesian Optimization and Semiparametric Models with Applications to Assistive Technology*. University of Toronto, 2013.
- [36] Jasper Snoek, Hugo Larochelle, and Ryan P Adams. Practical Bayesian optimization of machine learning algorithms. In *Advances in Neural Information Processing Systems 25*, pages 2951–2959. Curran Associates, Inc., 2012.
- [37] Shinya Suzuki, Shion Takeno, Tomoyuki Tamura, Kazuki Shitara, and Masayuki Karasuyama. Multi-objective Bayesian optimization using Pareto-frontier entropy. In *Proceedings of the 37th International Conference on Machine Learning*, volume 119, pages 9279–9288. PMLR, 2020.
- [38] Krister Svanberg. A class of globally convergent optimization methods based on conservative convex separable approximations. *SIAM J. on Optimization*, 12(2):555–573, 2002.
- [39] Shion Takeno, Hitoshi Fukuoka, Yuhki Tsukada, Toshiyuki Koyama, Motoki Shiga, Ichiro Takeuchi, and Masayuki Karasuyama. Multi-fidelity Bayesian optimization with max-value entropy search and its parallelization. In *Proceedings of the 37th International Conference on Machine Learning*, volume 119, pages 9334–9345. PMLR, 2020.

- [40] Julien Villemonteix, Emmanuel Vazquez, and Eric Walter. An informational approach to the global optimization of expensive-to-evaluate functions. *Journal of Global Optimization*, 44(4):509–534, 2009.
- [41] Zi Wang and Stefanie Jegelka. Max-value entropy search for efficient Bayesian optimization. In *Proceedings of the 34th International Conference on Machine Learning*, volume 70, pages 3627–3635. PMLR, 2017.
- [42] James Wilson, Frank Hutter, and Marc Deisenroth. Maximizing acquisition functions for Bayesian optimization. In *Advances in Neural Information Processing Systems 31*, page 9906–9917. Curran Associates, Inc., 2018.

A Definition of Gaussian processes

We use standard GP models [33] for modeling f and g_1, \dots, g_C . Suppose that the observations are contaminated with additive Gaussian noises as $y_{\mathbf{x}}^{(f)} = f(\mathbf{x}) + \varepsilon$ and $y_{\mathbf{x}}^{(g_c)} = g_c(\mathbf{x}) + \varepsilon$ for $\forall c$, where $\varepsilon \sim \mathcal{N}(0, \sigma_{\text{noise}}^2)$. For the GP prior, we employ $\mathcal{GP}(0, k(\mathbf{x}, \mathbf{x}'))$, which indicates that the prior mean is 0 and covariance is specified by a kernel function $k : \mathcal{X} \times \mathcal{X} \mapsto \mathbb{R}$. Then, the predictive distribution for $f(\mathbf{x})$ given $\mathcal{D}_n^{(f)} = \{(\mathbf{x}_i, y_{\mathbf{x}_i}^{(f)})\}_{i=1}^n$ is derived as follows:

$$\begin{aligned} f(\mathbf{x}) | \mathcal{D}_n^{(f)} &\sim \mathcal{N}(\mu_n^{(f)}(\mathbf{x}), \sigma_n^{(f)2}(\mathbf{x})), \\ \mu_n^{(f)}(\mathbf{x}) &= \mathbf{k}^\top (\mathbf{K} + \sigma_{\text{noise}}^2 \mathbf{I})^{-1} \mathbf{y}^{(f)}, \\ \sigma_n^{(f)2}(\mathbf{x}) &= k(\mathbf{x}, \mathbf{x}) - \mathbf{k}^\top (\mathbf{K} + \sigma_{\text{noise}}^2 \mathbf{I})^{-1} \mathbf{k}, \end{aligned}$$

where $\mathbf{y}^{(f)} = (y_{\mathbf{x}_1}^{(f)}, \dots, y_{\mathbf{x}_n}^{(f)})^\top$, $\mathbf{k} = (k(\mathbf{x}, \mathbf{x}_1), \dots, k(\mathbf{x}, \mathbf{x}_n))^\top$, $\mathbf{K} \in \mathbb{R}^{n \times n}$ is a kernel matrix whose (i, j) element is defined as $k(\mathbf{x}_i, \mathbf{x}_j)$, and $\mathbf{I} \in \mathbb{R}^{n \times n}$ is the identity matrix. The predictive distributions of g_c can be obtained in the same way using the observations $y_{\mathbf{x}_1}^{(g_c)}, \dots, y_{\mathbf{x}_n}^{(g_c)}$. Note that, for simplicity, we here assume the same kernels and noise variances for all the functions, but both the settings can be changed depending on the function.

B Derivation of information lower bound

Our information lower bound can be derived as follows:

$$\begin{aligned} I(\mathbf{h}_{\mathbf{x}}; f_*) &= \int \int p(\mathbf{h}_{\mathbf{x}}, f_*) \log \frac{p(\mathbf{h}_{\mathbf{x}}, f_*)}{p(\mathbf{h}_{\mathbf{x}})p(f_*)} d\mathbf{h}_{\mathbf{x}} df_* \\ &= \mathbb{E}_{f_*} \left[\int p(\mathbf{h}_{\mathbf{x}} | f_*) \log \frac{p(\mathbf{h}_{\mathbf{x}} | f_*)}{p(\mathbf{h}_{\mathbf{x}})} d\mathbf{h}_{\mathbf{x}} \right] \\ &= \mathbb{E}_{f_*} \left[\int p(\mathbf{h}_{\mathbf{x}} | f_*) \left(\log \frac{q(\mathbf{h}_{\mathbf{x}})}{p(\mathbf{h}_{\mathbf{x}})} + \log \frac{p(\mathbf{h}_{\mathbf{x}} | f_*)}{q(\mathbf{h}_{\mathbf{x}})} \right) d\mathbf{h}_{\mathbf{x}} \right] \\ &= \mathbb{E}_{f_*} \left[\int p(\mathbf{h}_{\mathbf{x}} | f_*) \log \frac{q(\mathbf{h}_{\mathbf{x}})}{p(\mathbf{h}_{\mathbf{x}})} d\mathbf{h}_{\mathbf{x}} + D_{\text{KL}}(p(\mathbf{h}_{\mathbf{x}} | f_*) || q(\mathbf{h}_{\mathbf{x}})) \right] \\ &\geq \mathbb{E}_{f_*} \left[\int p(\mathbf{h}_{\mathbf{x}} | f_*) \log \frac{q(\mathbf{h}_{\mathbf{x}})}{p(\mathbf{h}_{\mathbf{x}})} d\mathbf{h}_{\mathbf{x}} \right] \\ &= \mathbb{E}_{f_*} \left[\int p(\mathbf{h}_{\mathbf{x}} | f_*) \log \frac{p(\mathbf{h}_{\mathbf{x}} | \mathbf{h}_{\mathbf{x}} \in \overline{\mathcal{A}})}{p(\mathbf{h}_{\mathbf{x}})} d\mathbf{h}_{\mathbf{x}} \right]. \end{aligned} \tag{12}$$

In the last line, we replace $q(\mathbf{h}_{\mathbf{x}})$ with $p(\mathbf{h}_{\mathbf{x}} | \mathbf{h}_{\mathbf{x}} \in \overline{\mathcal{A}})$ as defined in (4). Here, from the definition of f_* , we see $p(\mathbf{h}_{\mathbf{x}} | f_*) = p(\mathbf{h}_{\mathbf{x}} | \mathbf{h}_{\mathbf{x}} \in \overline{\mathcal{A}}) = 0$ for $\mathbf{h}_{\mathbf{x}} \in \mathcal{A}$. Additionally, in information theory, $0 \log 0$ is treated as zero

based on that $\lim_{x \rightarrow 0} x \log x = 0$ [4]. Thus, we obtain

$$\begin{aligned}
(12) &= \mathbb{E}_{f_*} \left[\int_{\bar{\mathcal{A}}} p(\mathbf{h}_{\mathbf{x}} | f_*) \log \frac{p(\mathbf{h}_{\mathbf{x}})}{(1-Z)p(\mathbf{h}_{\mathbf{x}})} d\mathbf{h}_{\mathbf{x}} \right] \\
&= -\mathbb{E}_{f_*} \left[\int_{\bar{\mathcal{A}}} p(\mathbf{h}_{\mathbf{x}} | f_*) \log(1-Z) d\mathbf{h}_{\mathbf{x}} \right] \\
&= -\mathbb{E}_{f_*} \left[\log(1-Z) \int_{\bar{\mathcal{A}}} p(\mathbf{h}_{\mathbf{x}} | f_*) d\mathbf{h}_{\mathbf{x}} \right] \\
&= -\mathbb{E}_{f_*} [\log(1-Z)].
\end{aligned}$$

C Proof of Theorem 3.1 and Theorem 4.1

Let $f_{*(1)}, \dots, f_{*(K)}$ be i.i.d. random variables sampled from the distribution of f_* , and let $U_k := -\log(1 - \Pr(\mathbf{h}_{\mathbf{x}} \in \mathcal{A}_k))$, where $\mathcal{A}_k := (f_{*(k)}, \infty) \times (z_1, \infty) \times \dots \times (z_C, \infty)$ for $\forall k \in \{1, \dots, K\}$. Then, our acquisition function can be written as

$$\alpha_t^{\text{IBO}}(\mathbf{x}) = \frac{1}{K} \sum_{k=1}^K U_k.$$

We first show the variance of U_k is equal to or less than 2, i.e., $\mathbb{V}_{\mathcal{F}_*}[U_k] \leq 2$. For any $b \in \mathbb{R}$, the following inequality holds:

$$\Pr(\mathbf{h}_{\mathbf{x}} \in \mathcal{B}) \leq \Pr(f_* \geq b),$$

where $\mathcal{B} := (b, \infty) \times (z_1, \infty) \times \dots \times (z_C, \infty)$. This is because $f_* \geq f(\mathbf{x}) \geq b$ if $\mathbf{h}_{\mathbf{x}} \in \mathcal{B}$, which means \mathbf{x} is feasible and $f(\mathbf{x}) \geq b$. By substituting the sampled $f_{*(1)}, \dots, f_{*(K)}$ into b , we see

$$\Pr(\mathbf{h}_{\mathbf{x}} \in \mathcal{A}_k) \leq \Pr(f_* \geq f_{*(k)}).$$

From this inequality and the monotonicity of logarithm, we can transform

$$U_k = -\log(1 - \Pr(\mathbf{h}_{\mathbf{x}} \in \mathcal{A}_k)) \leq -\log(1 - \Pr(f_* \geq f_{*(k)})) = -\log(\Pr(f_* \leq f_{*(k)})) =: M_k.$$

U_k and M_k are nonnegative random variables, and $\Pr(U_k \leq M_k) = 1$. Hence, we see that $0 \leq \mathbb{E}_{\mathcal{F}_*}[U_k] \leq \mathbb{E}_{\mathcal{F}_*}[M_k]$ and $\mathbb{E}_{\mathcal{F}_*}[U_k^2] \leq \mathbb{E}_{\mathcal{F}_*}[M_k^2]$. Since f_* is a continuous random variable, we can apply the probability integral transform and its inverse transformation. Thus, the CDF $\Pr(f_* \leq f_{*(k)})$ follows a standard uniform distribution and its transformation by $-\log(\cdot)$ follows an exponential distribution with the rate parameter $\lambda = 1$:

$$\begin{aligned}
\Pr(f_* \leq f_{*(k)}) &\sim \text{Unif}(0, 1), \\
M_k = -\log(\Pr(f_* \leq f_{*(k)})) &\sim \exp(\lambda = 1).
\end{aligned}$$

Therefore, $\mathbb{E}_{\mathcal{F}_*}[M_k^2] = 2$. Consequently, we can derive the inequality below:

$$\begin{aligned}\mathbb{V}_{\mathcal{F}_*}[U_k] &= \mathbb{E}_{\mathcal{F}_*}[U_k^2] - \mathbb{E}_{\mathcal{F}_*}[U_k]^2 \\ &\leq \mathbb{E}_{\mathcal{F}_*}[U_k^2] \\ &\leq \mathbb{E}_{\mathcal{F}_*}[M_k^2] \\ &= 2.\end{aligned}$$

Our Monte Carlo estimator $\alpha_t^{\text{IBO}}(\mathbf{x})$ is unbiased, i.e., $\mathbb{E}_{\mathcal{F}_*}[\alpha_t^{\text{IBO}}(\mathbf{x})] = L(\mathbf{x})$, and thus, $\mathbb{E}_{\mathcal{F}_*}[(\alpha_t^{\text{IBO}}(\mathbf{x}) - L(\mathbf{x}))^2]$ is equal to the variance of $\alpha_t^{\text{IBO}}(\mathbf{x})$ with respect to the sampling of \mathcal{F}_* . Then, we derive

$$\begin{aligned}\mathbb{E}_{\mathcal{F}_*}[(\alpha_t^{\text{IBO}}(\mathbf{x}) - L(\mathbf{x}))^2] &= \mathbb{V}_{\mathcal{F}_*}\left[\frac{1}{K}\sum_{k=1}^K U_k\right] \\ &= \frac{1}{K^2}\mathbb{V}_{\mathcal{F}_*}\left[\sum_{k=1}^K U_k\right] \\ &= \frac{K}{K^2}\mathbb{V}_{\mathcal{F}_*}[U_k] \\ &\leq \frac{2}{K}.\end{aligned}$$

From above upper bound of the variance, we can obtain the following inequality as a direct consequence of the Chebyshev's inequality:

$$\Pr(|\alpha_t^{\text{IBO}}(\mathbf{x}) - L(\mathbf{x})| \geq \epsilon) \leq \frac{2/K}{\epsilon^2},$$

for any real number $\epsilon > 0$. By substituting $\Pr(|\alpha_t^{\text{IBO}}(\mathbf{x}) - L(\mathbf{x})| \geq \epsilon) = \delta$, the finite-sample bound of $|\alpha_t^{\text{IBO}}(\mathbf{x}) - L(\mathbf{x})|$ can be obtained as

$$|\alpha_t^{\text{IBO}}(\mathbf{x}) - L(\mathbf{x})| \leq \sqrt{\frac{2}{\delta K}},$$

with probability at least $1 - \delta$.

All the above derivations hold even after conditioning by \mathcal{H}_q for the parallel setting. Let $U_k^{(q)} := -\log(1 - \Pr(\mathbf{h}_{\mathbf{x}} \in \mathcal{A}_k | \mathcal{H}_{q-1}))$. Then, $\alpha_t^{\text{IBO}}(\mathbf{x} | \mathcal{X}_{q-1}) = 1/K \sum_{k=1}^K U_k^{(q)}$ and $U_k^{(q)} \leq M_k^{(q)} := -\log(\Pr(f_* \leq f_{*(k)} | \mathcal{H}_{q-1}))$ from the same derivation. Obviously, $M_k^{(q)}$ still follows the exponential distribution, and thus, $\mathbb{V}_{\mathcal{J}}[U_k^{(q)}] \leq 2$ still holds. The subsequent inequalities can be derived in the same way.

D Constrained max-value entropy search

We here extend cMES [28] to the multiple constraints setting and the parallel setting, and further, we show an example that its approximate MI can be negative.

D.1 Acquisition function of CMES

Following the conventional MES and cMES [41, 28], we transform and approximate MI as below:

$$\begin{aligned} (2) &= H(\mathbf{h}_x) - \mathbb{E}_{f_*} [H(\mathbf{h}_x | f_*)] \\ &\approx H(\mathbf{h}_x) - \mathbb{E}_{f_*} [H(\mathbf{h}_x | \mathbf{h}_x \in \bar{\mathcal{A}})]. \end{aligned} \quad (8)$$

For the approximation, the conditioning on f_* in the second term is replaced with $\mathbf{h}_x \in \bar{\mathcal{A}}$ following the existing approach [28]. Further, the expectation over $p(f_*)$ in the second term of (8) is also analytically intractable. This expectation can be approximated by the Monte Carlo method that samples f_* from $p(f_*)$, for which we employ the same RFF-based approach described in Appendix F.1. Thus, we obtain the following acquisition function as an approximation of (8):

$$\alpha_t^{\text{CMES}}(\mathbf{x}) := H(\mathbf{h}_x) - \frac{1}{K} \sum_{f_* \in \mathcal{F}_*} H(\mathbf{h}_x | \mathbf{h}_x \in \bar{\mathcal{A}}). \quad (13)$$

The first term is easy to calculate because it is the entropy of the multivariate normal distribution. Hence, we need to calculate the entropy in the second term $H(\mathbf{h}_x | \mathbf{h}_x \in \bar{\mathcal{A}})$.

Although Perrone et al. [28] derived a closed-form of the entropy of this TMN distribution specific for $C = 1$, for $C > 1$, directly evaluating it is not trivial as pointed out by [6]. We show that another analytical representation of this entropy actually can be derived for general C by transforming the domain of the integration as follows:

$$\begin{aligned} H(\mathbf{h}_x | \mathbf{h}_x \in \bar{\mathcal{A}}) &= \int_{\bar{\mathcal{A}}} -\frac{p(\mathbf{h}_x)}{1-Z} \log \frac{p(\mathbf{h}_x)}{1-Z} d\mathbf{h}_x \\ &= \int -\frac{p(\mathbf{h}_x)}{1-Z} \log \frac{p(\mathbf{h}_x)}{1-Z} d\mathbf{h}_x + \int_{\mathcal{A}} \frac{p(\mathbf{h}_x)}{1-Z} \log \frac{p(\mathbf{h}_x)}{1-Z} d\mathbf{h}_x \\ &= \frac{1}{1-Z} \int -p(\mathbf{h}_x) \log p(\mathbf{h}_x) d\mathbf{h}_x + \frac{1}{1-Z} \int_{\mathcal{A}} p(\mathbf{h}_x) \log p(\mathbf{h}_x) d\mathbf{h}_x + \log(1-Z) \\ &= \frac{1}{1-Z} \int -p(\mathbf{h}_x) \log p(\mathbf{h}_x) d\mathbf{h}_x + \frac{Z}{1-Z} \int_{\mathcal{A}} \frac{p(\mathbf{h}_x)}{Z} \log \frac{p(\mathbf{h}_x)}{Z} d\mathbf{h}_x + \log(1-Z) + \frac{Z \log(Z)}{1-Z} \\ &= \frac{H(\mathbf{h}_x)}{1-Z} - \frac{Z}{1-Z} \int_{\mathcal{A}} -p(\mathbf{h}_x | \mathbf{h}_x \in \mathcal{A}) \log p(\mathbf{h}_x | \mathbf{h}_x \in \mathcal{A}) d\mathbf{h}_x + \log(1-Z) + \frac{Z \log(Z)}{1-Z} \\ &= \frac{H(\mathbf{h}_x)}{1-Z} - \frac{ZH(\mathbf{h}_x | \mathbf{h}_x \in \mathcal{A})}{1-Z} + \log(1-Z) + \frac{Z \log Z}{1-Z}, \end{aligned} \quad (14)$$

where TMN $p(\mathbf{h}_x | \mathbf{h}_x \in \mathcal{A})$ is defined as

$$p(\mathbf{h}_x | \mathbf{h}_x \in \mathcal{A}) = \begin{cases} p(\mathbf{h}_x)/Z & \text{if } \mathbf{h}_x \in \mathcal{A} \\ 0 & \text{otherwise} \end{cases}.$$

In the last equation, Z and $H(\mathbf{h}_x)$ are easy to compute. Although $H(\mathbf{h}_x | \mathbf{h}_x \in \mathcal{A})$ in the second term is still the entropy of TMN, we show the calculation of this entropy in Appendix E for both independent and correlated cases.

Consequently, in the independent case, by substituting (14) into (13) and replacing $H(\mathbf{h}_{\mathbf{x}})$ and $H(\mathbf{h}_{\mathbf{x}} | \mathbf{h}_{\mathbf{x}} \in \mathcal{A})$ with their closed-forms (shown in Appendix E), we obtain

$$\alpha_t^{\text{CMES}}(\mathbf{x}) = \frac{1}{K} \sum_{f_* \in \mathcal{F}_*} \frac{Z}{2(1-Z)} R - \log(1-Z),$$

where

$$R := \frac{\gamma_t^{(f)}(\mathbf{x})\phi(\gamma_t^{(f)}(\mathbf{x}))}{1 - \Phi(\gamma_t^{(f)}(\mathbf{x}))} + \sum_{c=1}^C \frac{\gamma_t^{(g_c)}(\mathbf{x})\phi(\gamma_t^{(g_c)}(\mathbf{x}))}{1 - \Phi(\gamma_t^{(g_c)}(\mathbf{x}))}.$$

In the correlated case, $H(\mathbf{h}_{\mathbf{x}})$ and $H(\mathbf{h}_{\mathbf{x}} | \mathbf{h}_{\mathbf{x}} \in \mathcal{A})$ are also replaced with their closed-forms (shown in Appendix E), and we obtain

$$\alpha_t^{\text{CMES}}(\mathbf{x}) = \frac{1}{K} \sum_{f_* \in \mathcal{F}_*} \frac{Z}{2(1-Z)} \left(\text{Tr} \left(\boldsymbol{\Sigma}_{t-1}^{-1}(\mathbf{x}) (\boldsymbol{\Sigma}_{t-1}^{\text{TN}}(\mathbf{x}) + \mathbf{d}\mathbf{d}^\top) \right) - C - 1 \right) - \log(1-Z), \quad (15)$$

where $\text{Tr}(\cdot)$ is the trace of a matrix, and $\boldsymbol{\mu}_{t-1}(\mathbf{x})$ and $\boldsymbol{\Sigma}_{t-1}(\mathbf{x})$ are the expectation and covariance matrix of $\mathbf{h}_{\mathbf{x}}$, respectively, and $\boldsymbol{\mu}_{t-1}^{\text{TN}}(\mathbf{x})$ and $\boldsymbol{\Sigma}_{t-1}^{\text{TN}}(\mathbf{x})$ are those for $\mathbf{h}_{\mathbf{x}} | \mathbf{h}_{\mathbf{x}} \in \mathcal{A}$. See Appendix E for details.

D.2 Parallelization of CMES

We can consider the CMI maximization in the same way as CMES-IBO. Suppose that we already select the $q-1$ queries, and we need to select the next q -th query. The CMI can be approximated as

$$\begin{aligned} \mathbb{E}_{\mathcal{H}_{q-1}} [I(\mathbf{h}_{\mathbf{x}^{(q)}}; f_* | \mathcal{H}_{q-1})] &= \mathbb{E}_{\mathcal{H}_{q-1}} [H(\mathbf{h}_{\mathbf{x}^{(q)}} | \mathcal{H}_{q-1})] - \mathbb{E}_{\mathcal{H}_{q-1}, f_*} [H(\mathbf{h}_{\mathbf{x}^{(q)}} | f_*, \mathcal{H}_{q-1})] \\ &\approx \mathbb{E}_{\mathcal{H}_{q-1}} [H(\mathbf{h}_{\mathbf{x}^{(q)}} | \mathcal{H}_{q-1})] - \mathbb{E}_{\mathcal{H}_{q-1}, f_*} [H(\mathbf{h}_{\mathbf{x}^{(q)}} | \mathbf{h}_{\mathbf{x}^{(q)}} \in \bar{\mathcal{A}}, \mathcal{H}_{q-1})] \end{aligned}$$

As described in the main paper, we define $f(\mathbf{x}) | \mathcal{D}_{t-1}, \mathcal{X}_{q-1}, \mathcal{H}_{q-1} \sim \mathcal{N}(m_q^{(f)}(\mathbf{x}), s_q^{(f)2}(\mathbf{x}))$ and $g_c(\mathbf{x}) | \mathcal{D}_{t-1}, \mathcal{X}_{q-1}, \mathcal{H}_{q-1} \sim \mathcal{N}(m_q^{(g_c)}(\mathbf{x}), s_q^{(g_c)2}(\mathbf{x}))$ $c = 1, \dots, C$. Importantly, $s_q^{(f)2}(\mathbf{x}), s_q^{(g_c)2}(\mathbf{x}), \dots, s_q^{(g_C)2}(\mathbf{x})$ only depend on \mathcal{X}_{q-1} , not \mathcal{H}_{q-1} . Thus, given \mathcal{X}_{q-1} , the first term $\mathbb{E}_{\mathcal{H}_{q-1}} [H(\mathbf{h}_{\mathbf{x}^{(q)}} | \mathcal{H}_{q-1})]$ can be calculated analytically. The second term is also calculated in the same manner as CMES with given f_* and \mathcal{H}_{q-1} :

$$H(\mathbf{h}_{\mathbf{x}^{(q)}} | \mathbf{h}_{\mathbf{x}^{(q)}} \in \bar{\mathcal{A}}, \mathcal{H}_{q-1}) = H(\mathbf{h}_{\mathbf{x}^{(q)}} | \mathcal{H}_{q-1}) - \frac{Z_q}{2(1-Z_q)} R_q + \log(1-Z_q),$$

where

$$R_q := \frac{\eta_q^{(f)}(\mathbf{x}^{(q)})\phi(\eta_q^{(f)}(\mathbf{x}^{(q)}))}{1 - \Phi(\eta_q^{(f)}(\mathbf{x}^{(q)}))} + \sum_{c=1}^C \frac{\eta_q^{(g_c)}(\mathbf{x}^{(q)})\phi(\eta_q^{(g_c)}(\mathbf{x}^{(q)}))}{1 - \Phi(\eta_q^{(g_c)}(\mathbf{x}^{(q)}))}.$$

Finally, by applying the Monte Carlo approximation, we obtain the acquisition function below

$$\alpha_t^{\text{CMES}}(\mathbf{x}^{(q)} | \mathcal{X}_{q-1}) = \frac{1}{|\mathcal{J}|} \sum_{(f_*, \mathcal{H}_{q-1}) \in \mathcal{J}} \frac{Z_q}{2(1-Z_q)} R_q - \log(1-Z_q). \quad (16)$$

We can also derive the acquisition function in the correlated setting, but we omit the detailed derivation.

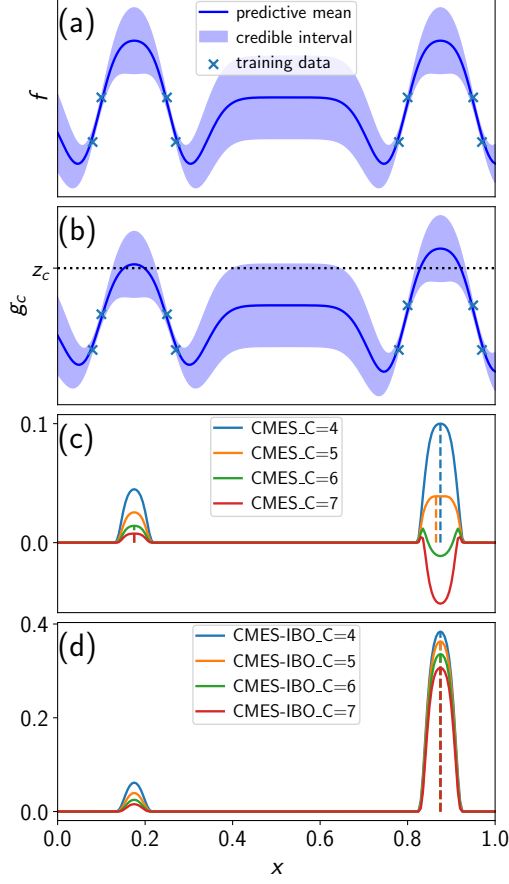


Figure 4: In (a) and (b), the predictions of f and g_c are shown, respectively. The solid line and shaded area represent the predictive mean and the credible interval, and the cross mark is the training data. The horizontal dotted line expresses z_c . In (c) and (d), the acquisition functions of CMES-IBO and CMES for $C = 4, 5, 6$, and 7 are shown, respectively. The vertical dotted lines represent the maximum of each acquisition function.

D.3 Illustrative example that CMES takes a negative value

Figure 4 shows an example that the approximate MI in CMES can be negative. We assume that all constraints g_1, \dots, g_C are the same function for simplicity. The plots (a) and (b) show the predictions of f and g_c , respectively. The plots (c) and (d) show the acquisition functions of CMES and CMES-IBO for $C = 4, 5, 6$, and 7 , respectively. We set $K = 10000$ and we sampled f_* as the maximum of function values drawn from the predictive multivariate normal distribution on the 200 equally spaced grid points. Thus, we expect that the sampling of f_* and the Monte Carlo estimation are highly accurate. However, in the case of $C = 6$ and 7 , we can clearly see that CMES takes negative values in the third plot. In this example, querying to the inputs around 0.2 and 0.9 are obviously beneficial because both of predictions of $f(\mathbf{x})$ and $g_c(\mathbf{x})$ are large. In particular, the inputs around 0.9 can be a better selection than around 0.2 because the probability of being feasible is the highest, while the uncertainty is almost the same as around 0.2. CMES-IBO selects a point

around 0.9 regardless of the number of constraints C . On the other hand, the acquisition function values of CMES for a point around 0.9 rapidly decrease with the number of constraints C . Although CMES selects a point around 0.9 for $C = 4$ and 5, but for $C = 6$ and 7, CMES selects a point around 0.2.

The possibility of negative values in CMES can also be seen analytically. By using $\log(1-Z) \geq (1 - \frac{1}{1-Z}) = \frac{-Z}{1-Z}$, an upper bound of the CMES acquisition function (9) can be derived as

$$\begin{aligned} & \frac{1}{K} \sum_{f_* \in \mathcal{F}_*} \left\{ \frac{Z}{2(1-Z)} \left(\frac{\gamma_t^{(f)}(\mathbf{x})\phi(\gamma_t^{(f)}(\mathbf{x}))}{1 - \Phi(\gamma_t^{(f)}(\mathbf{x}))} + \sum_{c=1}^C \frac{\gamma_t^{(g_c)}(\mathbf{x})\phi(\gamma_t^{(g_c)}(\mathbf{x}))}{1 - \Phi(\gamma_t^{(g_c)}(\mathbf{x}))} \right) - \log(1-Z) \right\} \\ & \leq \frac{1}{K} \sum_{f_* \in \mathcal{F}_*} \left\{ \frac{Z}{2(1-Z)} \left(\frac{\gamma_t^{(f)}(\mathbf{x})\phi(\gamma_t^{(f)}(\mathbf{x}))}{1 - \Phi(\gamma_t^{(f)}(\mathbf{x}))} + \sum_{c=1}^C \frac{\gamma_t^{(g_c)}(\mathbf{x})\phi(\gamma_t^{(g_c)}(\mathbf{x}))}{1 - \Phi(\gamma_t^{(g_c)}(\mathbf{x}))} \right) - \left(\frac{-Z}{1-Z} \right) \right\} \\ & = \frac{1}{K} \sum_{f_* \in \mathcal{F}_*} \frac{Z}{(1-Z)} \left\{ \frac{1}{2} \left(\frac{\gamma_t^{(f)}(\mathbf{x})\phi(\gamma_t^{(f)}(\mathbf{x}))}{1 - \Phi(\gamma_t^{(f)}(\mathbf{x}))} + \sum_{c=1}^C \frac{\gamma_t^{(g_c)}(\mathbf{x})\phi(\gamma_t^{(g_c)}(\mathbf{x}))}{1 - \Phi(\gamma_t^{(g_c)}(\mathbf{x}))} \right) + 1 \right\}. \end{aligned}$$

Let $a(\gamma) := \frac{\phi(\gamma)}{1-\Phi(\gamma)} \geq 0$. Since $\frac{Z}{1-Z} \geq 0$, we see that the sign of the above upper bound is determined by

$$\frac{1}{2} \gamma_t^{(f)}(\mathbf{x}) a(\gamma_t^{(f)}(\mathbf{x})) + \frac{1}{2} \sum_{c=1}^C \gamma_t^{(g_c)}(\mathbf{x}) a(\gamma_t^{(g_c)}(\mathbf{x})) + 1. \quad (17)$$

This equation clearly explains the behavior of CMES in Fig. 4. In the figure, we obviously see $\gamma_t^{(g_c)}(\mathbf{x}) = (z_c - \mu_{t-1}^{(g_c)}(\mathbf{x})) / \sigma_{t-1}^{(g_c)}(\mathbf{x}) < 0$ around $x = 0.9$. Since we now assume that g_c is same for $\forall c \in \{1, \dots, C\}$, the sign of (17) must be negative for sufficiently large C . Further, although we empirically observe that CMES can take negative values particularly for large C , the equation (17) shows that in principle, negative values can occur even for small C .

E Derivation of entropy of TMN

In this section, we derive the entropy of TMN truncated by a hyperrectangle $H(\mathbf{h}_x | \mathbf{h}_x \in \mathcal{A})$ for both independent and correlated cases.

E.1 Independent case

In this case, $H(\mathbf{h}_x | \mathbf{h}_x \in \mathcal{A})$ can be decomposed to the sum of the entropy of each element [19]:

$$H(\mathbf{h}_x | \mathbf{h}_x \in \mathcal{A}) = H(f(\mathbf{x}) | f(\mathbf{x}) \geq f_*) + \sum_{c=1}^C H(g_c(\mathbf{x}) | g_c(\mathbf{x}) \geq z_c).$$

The analytical form of the entropy of the one-dimensional truncated normal distribution is known [25], by which we obtain

$$\begin{aligned} H(f(\mathbf{x}) | f(\mathbf{x}) \geq f_*) &= \log(\sqrt{2\pi}e\sigma_{t-1}^{(f)}(\mathbf{x})(1 - \Phi(\gamma_t^{(f)}(\mathbf{x}))) + \frac{\gamma_t^{(f)}(\mathbf{x})\phi(\gamma_t^{(f)}(\mathbf{x}))}{2(1 - \Phi(\gamma_t^{(f)}(\mathbf{x})))}, \\ H(g_c(\mathbf{x}) | g_c(\mathbf{x}) \geq z_c) &= \log(\sqrt{2\pi}e\sigma_{t-1}^{(g_c)}(\mathbf{x})(1 - \Phi(\gamma_t^{(g_c)}(\mathbf{x}))) + \frac{\gamma_t^{(g_c)}(\mathbf{x})\phi(\gamma_t^{(g_c)}(\mathbf{x}))}{2(1 - \Phi(\gamma_t^{(g_c)}(\mathbf{x})))}. \end{aligned}$$

Moreover, we see $H(\mathbf{h}_x) = \log(\sqrt{2\pi}e\sigma_{t-1}^{(f)}(\mathbf{x})) + \sum_{c=1}^C \log(\sqrt{2\pi}e\sigma_{t-1}^{(g_c)}(\mathbf{x}))$ from the independence of each elements of \mathbf{h}_x . Then, the entropy of TMN is obtained as

$$H(\mathbf{h}_x|\mathbf{h}_x \in \mathcal{A}) = H(\mathbf{h}_x) + \log(Z) + \frac{R}{2},$$

where

$$R = \frac{\gamma_t^{(f)}(\mathbf{x})\phi(\gamma_t^{(f)}(\mathbf{x}))}{1 - \Phi(\gamma_t^{(f)}(\mathbf{x}))} + \sum_{c=1}^C \frac{\gamma_t^{(g_c)}(\mathbf{x})\phi(\gamma_t^{(g_c)}(\mathbf{x}))}{1 - \Phi(\gamma_t^{(g_c)}(\mathbf{x}))}.$$

E.2 Correlated case

Supposed that \mathbf{h}_x has a correlated distribution defined as

$$\mathbf{h}_x|\mathcal{D}_{t-1} \sim \mathcal{N}(\boldsymbol{\mu}_{t-1}(\mathbf{x}), \boldsymbol{\Sigma}_{t-1}(\mathbf{x})),$$

where $\boldsymbol{\mu}_{t-1}(\mathbf{x})$ and $\boldsymbol{\Sigma}_{t-1}(\mathbf{x})$ can be obtained by an arbitrary multi-output GP model [33]. Let $\boldsymbol{\mu}_{t-1}^{\text{TN}}(\mathbf{x})$ and $\boldsymbol{\Sigma}_{t-1}^{\text{TN}}(\mathbf{x})$ be the expectation and covariance matrix of $\mathbf{h}_x|\mathbf{h}_x \in \mathcal{A}$, respectively, whose analytical expressions are known [7]. We denote $\mathbb{E}_{\mathbf{h}_x|\mathbf{h}_x \in \mathcal{A}}$, which is the expectation with respect to $\mathbf{h}_x|\mathbf{h}_x \in \mathcal{A}$, as \mathbb{E}_{TN} for brevity.

Then, we can transform the entropy $H(\mathbf{h}_x|\mathbf{h}_x \in \mathcal{A})$ into

$$\begin{aligned} H(\mathbf{h}_x|\mathbf{h}_x \in \mathcal{A}) &= \mathbb{E}_{\text{TN}} \left[-\log p(\mathbf{h}_x|\mathbf{h}_x \in \mathcal{A}) \right] \\ &= \mathbb{E}_{\text{TN}} \left[-\log \frac{p(\mathbf{h}_x)}{Z} \right] \\ &= \mathbb{E}_{\text{TN}} [-\log p(\mathbf{h}_x)] + \log Z \\ &= \frac{1}{2} \mathbb{E}_{\text{TN}} [(\mathbf{h}_x - \boldsymbol{\mu}_{t-1}(\mathbf{x}))^\top \boldsymbol{\Sigma}_{t-1}^{-1}(\mathbf{x})(\mathbf{h}_x - \boldsymbol{\mu}_{t-1}(\mathbf{x}))] + \frac{1}{2} |2\pi \boldsymbol{\Sigma}_{t-1}(\mathbf{x})| + \log Z \\ &= \frac{1}{2} \text{Tr} \left(\underbrace{\boldsymbol{\Sigma}_{t-1}^{-1}(\mathbf{x}) \mathbb{E}_{\text{TN}} [(\mathbf{h}_x - \boldsymbol{\mu}_{t-1}(\mathbf{x}))(\mathbf{h}_x - \boldsymbol{\mu}_{t-1}(\mathbf{x}))^\top]}_{=: \mathbf{V}} \right) + \frac{1}{2} |2\pi \boldsymbol{\Sigma}_{t-1}(\mathbf{x})| + \log Z, \end{aligned}$$

where $|\cdot|$ is the determinant of a matrix. Further, by using $\mathbf{d} = \boldsymbol{\mu}_{t-1}^{\text{TN}}(\mathbf{x}) - \boldsymbol{\mu}_{t-1}(\mathbf{x})$, we obtain

$$\begin{aligned} \mathbf{V} &= \mathbb{E}_{\text{TN}} [(\mathbf{h}_x - \boldsymbol{\mu}_{t-1}^{\text{TN}}(\mathbf{x}) + \mathbf{d})(\mathbf{h}_x - \boldsymbol{\mu}_{t-1}^{\text{TN}}(\mathbf{x}) + \mathbf{d})^\top] \\ &= \mathbb{E}_{\text{TN}} [(\mathbf{h}_x - \boldsymbol{\mu}_{t-1}^{\text{TN}}(\mathbf{x}))(\mathbf{h}_x - \boldsymbol{\mu}_{t-1}^{\text{TN}}(\mathbf{x}))^\top + \mathbf{d}(\mathbf{h}_x - \boldsymbol{\mu}_{t-1}^{\text{TN}}(\mathbf{x}))^\top + (\mathbf{h}_x - \boldsymbol{\mu}_{t-1}^{\text{TN}}(\mathbf{x}))\mathbf{d}^\top + \mathbf{d}\mathbf{d}^\top] \\ &= \mathbb{E}_{\text{TN}} [(\mathbf{h}_x - \boldsymbol{\mu}_{t-1}^{\text{TN}}(\mathbf{x}))(\mathbf{h}_x - \boldsymbol{\mu}_{t-1}^{\text{TN}}(\mathbf{x}))^\top] + \mathbf{d}\mathbf{d}^\top \\ &= \boldsymbol{\Sigma}_{t-1}^{\text{TN}}(\mathbf{x}) + \mathbf{d}\mathbf{d}^\top, \end{aligned}$$

where we use $\mathbb{E}_{\text{TN}} [(\mathbf{h}_x - \boldsymbol{\mu}_{t-1}^{\text{TN}}(\mathbf{x}))] = 0$. Consequently, we can derive

$$H(\mathbf{h}_x|\mathbf{h}_x \in \mathcal{A}) = \frac{1}{2} \text{Tr} \left(\boldsymbol{\Sigma}_{t-1}^{-1}(\mathbf{x})(\boldsymbol{\Sigma}_{t-1}^{\text{TN}}(\mathbf{x}) + \mathbf{d}\mathbf{d}^\top) \right) + \frac{1}{2} |2\pi \boldsymbol{\Sigma}_{t-1}(\mathbf{x})| + \log Z.$$

Algorithm 1 Sequential- and parallel- CMES-IBO.

```

1: function CMES-IBO( $\mathcal{D}_0, \mathcal{X}, Q, K, \zeta$ )
2:   for  $t = 0, \dots, T$  do
3:     for  $k = 1, \dots, K$  do
4:       Sample  $\tilde{f}_{(k)}, \tilde{g}_{1(k)}, \dots, \tilde{g}_{C(k)}$  from current GPs
5:        $f_{*(k)} \leftarrow \begin{cases} \max_{\mathbf{x} \in \tilde{\mathcal{X}}_{\text{feasible}}} \tilde{f}_{(k)}(\mathbf{x}), & \text{if } \tilde{\mathcal{X}}_{\text{feasible}} \neq \emptyset, \\ \min_{\mathbf{x} \in \mathcal{X}} \tilde{f}_{(k)}(\mathbf{x}) - \zeta, & \text{otherwise,} \end{cases}$ 
        where  $\tilde{\mathcal{X}}_{\text{feasible}} := \{\mathbf{x} \mid \tilde{g}_c(\mathbf{x}) \geq z_c, c = 1, \dots, C\}$ 
6:     end for
7:      $\mathcal{F}_* = \{f_{*(k)}\}_{k=1}^K$ 
8:      $\mathbf{x}_t^{(1)} \leftarrow \arg \max_{\mathbf{x} \in \mathcal{X}} \alpha_t^{\text{IBO}}(\mathbf{x})$  (7)
9:     if  $Q > 1$  then
10:      for  $q = 2, \dots, Q$  do
11:         $\mathcal{J} = \left\{ \left( f_{*(k)}, \left\{ \left( \tilde{f}_{(k)}(\mathbf{x}_t^{(q')}), \tilde{g}_{1(k)}(\mathbf{x}_t^{(q')}), \dots, \tilde{g}_{C(k)}(\mathbf{x}_t^{(q')}) \right)^\top \right\}_{q'=1}^{q-1} \right) \right\}_{k=1}^K$ 
12:         $\mathbf{x}_t^{(q)} \leftarrow \arg \max_{\mathbf{x} \in \mathcal{X}} \alpha_t^{\text{IBO}}(\mathbf{x} | \mathcal{X}_{q-1})$  (11)
13:      end for
14:    end if
15:    Evaluate  $f, g_1, \dots, g_C$  at  $\mathcal{X}_q$ 
16:    Update  $\mathcal{D}_t^{(f)}, \mathcal{D}_t^{(g_1)}, \dots, \mathcal{D}_t^{(g_C)}$  adding new observations
17:  end for
18: end function

```

F Computation of CMES and CMES-IBO

In this section, we describe several computational details. First, we present the general algorithm for sequential- and parallel- CMES-IBO in Algo. 1, where sequential CMES-IBO corresponds to the case that $Q = 1$. By replacing (7) and (11) in Algo. 1 with those of CMES (9) and (16), this algorithm can also be seen as the algorithm for sequential- and parallel- CMES.

F.1 Sampling from posterior

Our proposed method needs to sample the maximum value f_* defined by (1). We employ an approach using random Fourier features (RFF) [32], which has been used in various entropy-based BO and CBO methods [15, 16, 41]. In the RFF-based sampling, RFF $\phi(\mathbf{x}) \in \mathbb{R}^D$ are first generated, and a Bayesian linear regression model $f(\mathbf{x}) \approx \boldsymbol{\omega}^\top \phi(\mathbf{x})$ with the coefficients $\boldsymbol{\omega} \in \mathbb{R}^D$ is constructed. By sampling the coefficients $\boldsymbol{\omega}$ from the Gaussian posterior, a continuous sample path can be derived. Let $\tilde{f}_{(k)}$ and $\tilde{g}_{c(k)}$ ($c \in \{1, \dots, C\}$) be the k -th set of sample paths ($k \in \{1, \dots, K\}$) for the objective and constraint functions. The k -th sample of f_* , can be obtained by solving a constrained optimization problem $\max_{\mathbf{x} \in \mathcal{X}} \tilde{f}_{(k)}(\mathbf{x})$, s.t. $\tilde{g}_{c(k)}(\mathbf{x}) \geq z_c$, $c = 1, \dots, C$.

We can apply any constrained optimization modules such as the method of moving asymptotes [38]. Another approach would be the discretization-based sampling through multivariate normal distribution [28], though the number of discretization points strongly depends on the input dimension d for sufficiently accurate sampling.

For parallel querying, we need to sample the f_* and \mathcal{H}_{q-1} simultaneously. By using RFF-based sampling, these random variables are sampled from a joint distribution easily, i.e., \mathcal{H}_{q-1} can be sampled as a value of the sample paths $\tilde{f}_{(k)}(\mathbf{x})$ and $\tilde{g}_{c(k)}(\mathbf{x})$ at $\mathbf{x} \in \mathcal{X}_{q-1}$. Moreover, in the Monte Carlo approximation for $q > 1$, we can reuse the sample paths $\tilde{f}_{(k)}, \tilde{g}_{1(k)}, \dots, \tilde{g}_{C(k)}$ that are sampled at $q = 1$ as described in Algo. 1. Because of this reuse, the computational cost of parallel CMES and CMES-IBO are much smaller than Q times that of sequential CMES and CMES-IBO, respectively.

F.2 Computational complexity of CMES-IBO and CMES

Independent Case To generate sample paths, the Bayesian linear regression requires $O(CKD^3)$ for the given RFF, but C, K and D are usually not large values. The number of constraints C is often less than 10. In our empirical observations, the performance of CMES-IBO were stable with a small number of Monte Carlo samplings K such as 10. The dimension of the RFF features D is typically set as less than 1000. The complexity for solving the generated constraint problems depends on the solver. Many gradient-based methods have been known for the white-box constrained optimization such as the sequential quadratic programming and the interior point method. The gradient of a sample path can be obtained by $O(dD)$, and thus, those gradient-based solvers can be applied efficiently.

Once we obtain the samples of f_* , the acquisition functions CMES-IBO (7) and CMES (9) can be easily calculated for $\forall \mathbf{x}$ by using the GP posterior of f and g_c . Since we employ a standard GP model, the posterior can be computed with $O(n^3)$ for a given kernel matrix, where n is the number of the observed points. Note that the $O(n^3)$ computation is required only once through the acquisition function maximization, because by storing $(\mathbf{K} + \sigma_{\text{noise}}^2 \mathbf{I})^{-1}$, the predictive mean and variance can be evaluated by $O(n^2)$ for a given \mathbf{x} . In our setting, the function evaluation is assumed to be expensive, by which we usually only have a moderate size of a training set (typically, at most several hundreds of points).

In the case of the parallel setting, we need $m_q^{(f)}$ and $s_q^{(f)2}$, which are the predictive mean and variance of $f(\mathbf{x})$ after conditioning \mathcal{H}_{q-1} . This conditional density is written as $p(f(\mathbf{x}) | \tilde{f}_{(k)}(\mathbf{x}^{(1)}), \dots, \tilde{f}_{(k)}(\mathbf{x}^{(q-1)}))$, which can be easily determined through the standard conditional Gaussian formula. Given the $q \times q$ predictive covariance matrix of the current GP for \mathbf{x} and \mathcal{X}_{q-1} , we can obtain $m_q^{(f)}(\mathbf{x})$ and $s_q^{(f)2}(\mathbf{x})$ with $O(q^3)$. For $m_q^{(g_c)}$ and $s_q^{(g_c)2}$, which are for constraint functions, the same calculation can be applied.

Correlated Case For CMES-IBO and CMES, the computations of CDF of the multivariate normal distribution are needed in the correlated case, as shown in Appendix E.2. CMES-IBO performs K times $C + 1$ dimensional CDF for the acquisition function (7), in which $Z = \Pr(\mathbf{h} \in \mathcal{A})$ is now CDF of a correlated

multivariate normal distribution. On the other hand, in addition to these CDF computations, CMES performs K times computations of the expectation and covariance matrix of TMN in the acquisition function (15), each of which needs computing C dimensional CDF $C + 1$ times and $C - 1$ dimensional CDF $C(C + 1)/2$ times, respectively [7]. Using a well-known Monte Carlo-based algorithm [10], the computational complexity of CDF with respect to the dimension C is known to be $O(C^2)$. Therefore, the computational complexity of CMES-IBO with respect to K and C is $O(KC^2)$, but that of CMES is $O(KC^4)$, which severely limits the applicability of CMES to the large number of constraints.

G Considerations on regret bound of MES

In this section, we describe flaws in the theoretical analysis of MES [41]. We use the same notation as [41] throughout this section. Wang and Jegelka [41] showed the bound of simple regret $r_T := \max_{\mathbf{x} \in \mathcal{X}} f(\mathbf{x}) - \max_{t \in [1, T]} f(\mathbf{x}_t)$ as follows:

Theorem G.1 (Theorem 3.2 in [41]). *Let F be the cumulative probability distribution for the maximum of any function f sampled from $GP(\mu, k)$ over the compact search space $\mathcal{X} \subset \mathbb{R}^d$, where $k(\mathbf{x}, \mathbf{x}') \leq 1, \forall \mathbf{x}, \mathbf{x}' \in \mathcal{X}$. Let $f_* = \max_{\mathbf{x} \in \mathcal{X}} f(\mathbf{x})$ and $w = F(f_*) \in (0, 1)$, and assume the observation noise is iid $\mathcal{N}(0, \sigma^2)$. If in each iteration t , the query point is chosen as $\mathbf{x}_t = \arg \max_{\mathbf{x} \in \mathcal{X}} \gamma_{y_*^t}(\mathbf{x}) \frac{\psi(\gamma_{y_*^t}(\mathbf{x}))}{2\Psi(\gamma_{y_*^t}(\mathbf{x}))} - \log(\Psi(\gamma_{y_*^t}(\mathbf{x})))$, where $\gamma_{y_*^t}(\mathbf{x}) = \frac{y_*^t - \mu_t(\mathbf{x})}{\sigma_t(\mathbf{x})}$ and y_*^t is drawn from F , then with probability at least $1 - \delta$, in $T' = \sum_{i=1}^T \log_w \frac{\delta}{2\pi_i}$ number of iterations, the simple regret satisfies*

$$r_{T'} \leq \sqrt{\frac{C\rho_T}{T}}(\nu_{t^*} + \zeta_T), \quad (18)$$

where $C = 2/\log(1 + \sigma^{-2})$ and $\zeta_T = (2 \log(\frac{\pi_T}{\delta}))^{\frac{1}{2}}$, π_i satisfies $\sum_{i=1}^T \pi_i^{-1} \leq 1$ and $\pi_t > 0$, and $t^* = \arg \max_t \nu_t$ with $\nu_t \triangleq \min_{\mathbf{x} \in \mathcal{X}, y_*^t > f_*} \gamma_{y_*^t}(\mathbf{x})$, and ρ_T is the maximum information gain of at most T selected points.

In this theorem, the simple regret for ‘one sample MES’ is analyzed, in which only one max-value is sampled at every iteration in the algorithm. We summarize five main flaws in this theorem as follows (note that each of them is related to each other):

1. From the assumption $f \sim \mathcal{GP}(\mu, k)$, the max-value f_* is a random variable, but it is not treated as a random variable in their analysis. For example, Lemma C.1 in [41] obviously assumes that $f(\mathbf{x}_t)$ follows the Gaussian distribution, and therefore, treating f_* as a deterministic variable contradicts the assumption of this lemma. This problem closely related to other flaws, and thus, it is difficult to correct.
2. In BO literature, usually, the number of iterations is represented by T , and Wang and Jegelka [41] use this notation except for the theorem. On the other hand, in the theorem, the number of iteration is represented by T' instead of T , and the variable T in the bound (18) is defined by the number of ‘partitioning’ of the entire iterations in their proof. Each partition is defined so that it satisfies a probabilistic condition related to max-values, which we omit details here. An important issue is that,

for this replaced T , dependency on the actual number of iterations is not clarified. Therefore, (18) does not reveal the convergence rate with respect to the number of iterations.

3. Since ν_{t^*} depends on y_*^t in each iteration, ν_{t^*} is a random variable. This variable remains in the final upper bound, but the convergence rate of ν_{t^*} has not been shown.
4. In the theorem, Wang and Jegelka [41] assumed that y_*^t is drawn from the prior F . This assumption clearly does not match the basic idea of MES that selects the next query based on the mutual information estimated through samples of the max-value from the ‘posterior’ distribution.
5. Wang and Jegelka [41] claimed that the above simple regret bound can adapt to the setting that y_*^t is drawn from the posterior. However, this claim is not proven and not obvious. In the proof, Wang and Jegelka [41] implicitly assumed $\Pr(y_*^t < f_*, y_*^{t+1} < f_*) = \Pr(y_*^t < f_*) \Pr(y_*^{t+1} < f_*)$. Through the basic formula of the joint probability of independent variables, this decomposition is allowed if f_* is deterministic, and y_*^t and y_*^{t+1} are independent of each other. However, both of these two conditions are not satisfied in the case of sampling from the posterior. For the first condition, as we already mention, f_* should be a random variable (actually, this first condition is not satisfied even for the case of sampling from the prior). For the second condition, when y_*^t and y_*^{t+1} are sampled from posterior, y_*^t depends on \mathcal{D}_{t-1} and y_*^{t+1} depends on \mathcal{D}_t . However, since $\mathcal{D}_{t-1} \subset \mathcal{D}_t$, dependency obviously exists between y_*^t and y_*^{t+1} (note that now \mathcal{D}_{t-1} and \mathcal{D}_t are also random variables not only because of the random noise of observations, but also the randomness in the acquisition function). In the proof, the decomposition is not justified when the two conditions are not satisfied. This decomposition plays a key role in the proof, and we consider that the above issue is not easy to avoid.

We first tried to extend this theorem to our constrained problem, but we consider that correcting the above issues is at least not trivial. Therefore, theoretical analysis of the MES-based methods (even for the simple unconstrained case) is still an open problem, to the best of our knowledge.

H Details of experimental settings

In this section, we describe additional details of experimental settings.

H.1 Other experimental settings for benchmark functions

Observations for objective and constraint functions are standardized so that they have zero mean and unit variance, respectively, before the regression at every iteration. We used the open-source library called GPpy [11] for the GP regression. The candidate intervals of hyperparameters σ_{LIN}^2 and σ_{RBF}^2 are set to $[0, 1]$, and the variance of the noise σ^2 is set to 10^{-6} . As we mentioned in the main paper, other hyperparameters are chosen by marginal likelihood maximization. We employed an Automatic Relevance Determination (ARD)

for the RBF kernel. Thus, the RBF kernel has a hyperparameter $\boldsymbol{\ell} := (\ell_1, \dots, \ell_d)^\top \in \mathbb{R}^d$, and it is written as

$$k_{\text{RBF}}(\mathbf{x}, \mathbf{x}') := \exp\left(-\frac{1}{2} \sum_{i=1}^d \frac{(x_i - x'_i)^2}{\ell_i^2}\right),$$

where x_i and x'_i are the i -th elements of \mathbf{x} and \mathbf{x}' , respectively. For each one of ℓ_i for $i = 1, \dots, d$, we set the same interval of the candidate value. For benchmark functions, we set $\ell_i \in [10^{-1}s, 10s]$, where s is the length of the interval for the possible value of x_i in the input domain, which is identical for $\forall i$ in the benchmark functions. For all benchmark functions, $z_c = 0$ for $c = 1, \dots, C$. We used the method of moving asymptotes [38] in NLOpt [20] for the constrained optimization of the sample path in CMES-IBO, CMES, TSC and their parallel extensions. Finally, the hyperparameter M of P-EIC is selected as the minimum of the current observations.

H.2 Details of benchmark functions

Here, we provide detailed information on benchmark functions. Note that we change the sign from the original functions if it is required to formalize as the maximization problem.

Gardner1 Gardner1 is a simple test problem in which functions are constructed by sine and cosine functions [8]. The input dimension $d = 2$, the input domain $\mathcal{X} = [0, 6]^2$, and the number of constraints $C = 1$. The detailed forms of functions are

$$\begin{aligned} f(\mathbf{x}) &= -\cos(2x_1) \cos(x_2) - \sin(x_1), \\ g_1(\mathbf{x}) &= -\cos(x_1) \cos(x_2) + \sin(x_1) \sin(x_2) + 0.5. \end{aligned}$$

Gardner2 Gardner2 also has a simple form, but its feasible region is very small [8]. The input dimension $d = 2$, the input domain $\mathcal{X} = [0, 6]^2$, and the number of constraints $C = 1$. The detailed forms of functions are

$$\begin{aligned} f(\mathbf{x}) &= -\sin(x_1) - x_2, \\ g_1(\mathbf{x}) &= -\sin(x_1) \sin(x_2) - 0.95. \end{aligned}$$

Gramacy The Gramacy function is from [13]. The input dimension $d = 2$, the input domain $\mathcal{X} = [0, 1]^2$, and the number of constraints $C = 2$. The detailed forms of functions are

$$\begin{aligned} f(\mathbf{x}) &= -x_1 - x_2, \\ g_1(\mathbf{x}) &= \frac{1}{2} \sin(2\pi(x_1^2 - 2x_2)) + x_1 + 2x_2 - 1.5, \\ g_2(\mathbf{x}) &= -x_1^2 - x_2^2 + 1.5. \end{aligned}$$

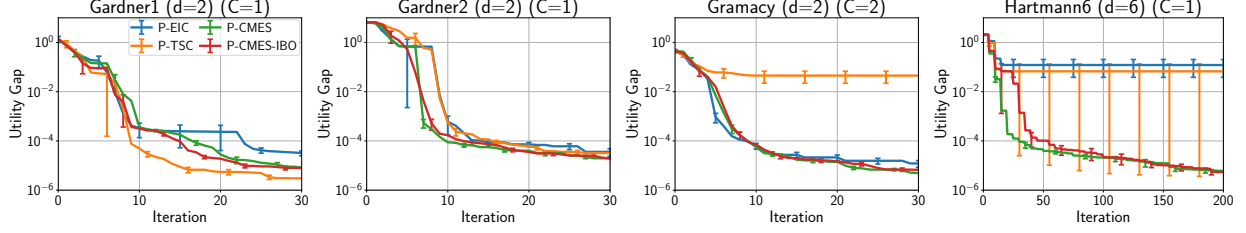


Figure 5: Utility gap of benchmark functions (average and standard error).

Hartmann6 The Hartmann6 function is used in [22]. The input dimension $d = 6$, the input domain $\mathcal{X} = [0, 1]^6$, and the number of constraints $C = 1$. The detailed forms of functions are

$$f(\mathbf{x}) = \sum_{i=1}^4 \alpha_i \exp\left(-\sum_{j=1}^6 A_{ij}(x_j - P_{ij})^2\right),$$

$$g_1(\mathbf{x}) = -\|\mathbf{x} - \mathbf{x}'\| + 1,$$

where

$$\boldsymbol{\alpha} = (1.0, 1.2, 3.0, 3.2)^\top,$$

$$\mathbf{A} = \begin{pmatrix} 10 & 3 & 17 & 3.5 & 1.7 & 8 \\ 0.05 & 10 & 17 & 0.1 & 8 & 14 \\ 3 & 3.5 & 1.7 & 10 & 17 & 8 \\ 17 & 8 & 0.05 & 10 & 0.1 & 14 \end{pmatrix},$$

$$\mathbf{P} = 10^{-4} \begin{pmatrix} 1312 & 1696 & 5569 & 124 & 8283 & 5886 \\ 2329 & 4135 & 8307 & 3736 & 1004 & 9991 \\ 2348 & 1451 & 3522 & 2883 & 3047 & 6650 \\ 4047 & 8828 & 8732 & 5743 & 1091 & 381 \end{pmatrix}.$$

I Additional experiments

I.1 Experiments on small C problems for the parallel setting

Here, we show the experimental results of benchmark functions on the parallel setting in Fig. 5. In the Gardner2, Gramacy, and Hartmann6 functions, CMES-IBO and CMES showed the best or comparable to the best results. TSC showed better performance in the Gardner1 function, but it was stagnated in the Gramacy and Hartmann6 functions.

I.2 Experiments on large C problems

The results on the three benchmark functions called G1 ($d = 13$ and $C = 9$), G4 ($d = 5$ and $C = 6$), and G9 ($d = 7$ and $C = 4$) are shown in Fig. 6. For the sequential querying, CMES-IBO was the best or comparable

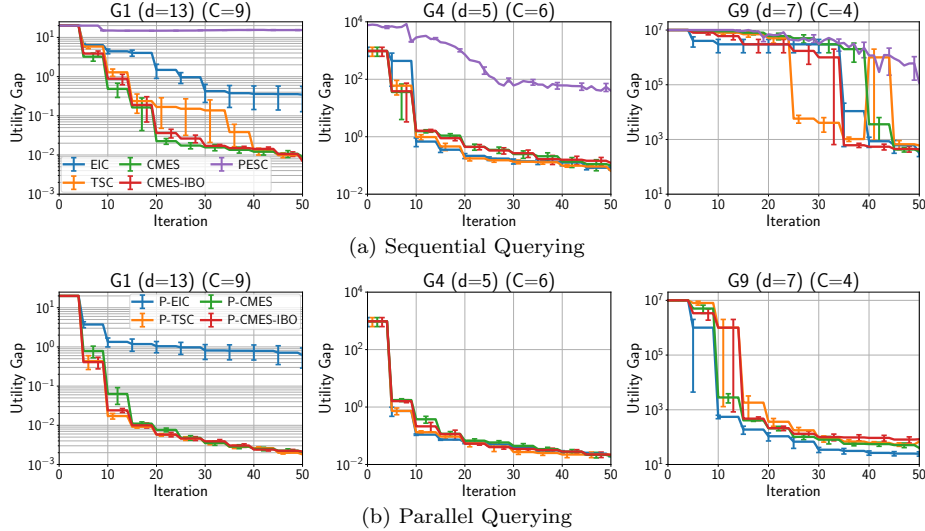


Figure 6: Utility gap of G1, G4, and G9 functions (average and standard error).

to the best methods in all the results. In G9, TSC decreased the gap rapidly, but it showed the unstable behavior from the iterations around 40 to 45. The instability of TSC can also be seen in G1 at the iteration around 30. We consider that these unstable behavior stem from the stochastic nature of TSC. EIC was slow for G1 though the other benchmark functions, it shows reasonable performance. For the parallel querying, CMES-IBO again showed stable performance, though most of the methods have similar performance in these cases.

I.3 Experiment for correlated synthetic function

We evaluate the performance of CMES-IBO with correlated GPs on synthetic functions ($d = 3$ and $C = 3$). Because of its high computational complexity, we did not employ CMES here (see Appendix F.2). The objective and $C = 3$ constraints were sampled from GPs with the RBF kernel, and the length scales of the kernels were 0.1. All the correlation coefficients among the objective and constraint functions were set as 0.5. The same settings of GPs for the function generation were also used in each BO method. The threshold for constraints were set as $z_c = 0$ for $\forall c$, and the input domain was $[0, 1]^3$. We sampled 5 sets of functions, and the experiment of each set ran 10 times. We report the mean and standard error of these 50 trials. Figure 7 shows the result. C-CMES-IBO denotes the correlated extension of CMES-IBO. We see that C-CMES-IBO improves CMES-IBO in this case and superior to the other methods. Although the correlated model can improve performance when the true function has strong correlation, we mainly focus on the independent setting because the efficiency is often comparable to the correlated model and the computations of independent CMES-IBO is much simpler than correlated case.

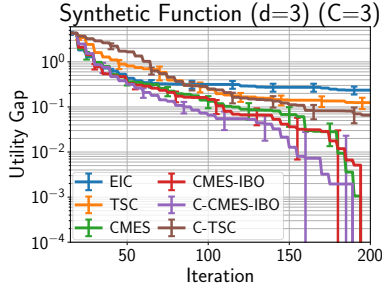


Figure 7: Utility gap of correlated GP-derived synthetic functions (average and standard error).

Table 1: Computational time (sec.) for the Gramacy function at $t = 30$ (mean \pm standard error)

	sampling of f_*	optimization of $\alpha(\mathbf{x})$
EIC	NA	1.148 ± 0.287
TSC	NA	2.670 ± 0.464
CMES	20.728 ± 1.498	0.780 ± 1.317
CMES-IBO	21.836 ± 0.933	1.163 ± 2.130

I.4 Experiment for computational time evaluation

In Table 1, we evaluate computational time of the acquisition function maximization at $t = 30$. EIC and TSC were relatively faster than the others. CMES-IBO and CMES took longer times because of sampling of f_* for which we need to solve constraint optimization problems K times, while the acquisition function maximization itself was fast enough because of their simple closed forms of the acquisition functions. Although it is not shown here, PESC has the same computational requirement for sampling x_* because the same constraint optimization problems need to be solved. It is worth noting that the K times sampling of f_* can be accelerated by computing in parallel because each one of the samplings is independent.